Asymmetry Between Galaxy Apparent Magnitudes Shows a Possible Tension Between Physical Properties of Galaxies and their Rotational Velocity

Darius McAdam, Lior Shamir*
Kansas State University
1701 Platt St
Manhattan, KS 66506, USA

Abstract

Despite over a century of research, the physics of galaxy rotation is not yet fully understood, with clear discrepancy between the observed mass of galaxies and their rotational velocity. Here we report on another observation of tension between the physical properties of galaxies and their rotational velocity. We compare the apparent magnitude of galaxies, and find a statistically significant asymmetry between galaxies that rotate in the same direction relative to the Milky Way and galaxies that rotate in the opposite direction relative to the Milky Way. While asymmetry in the brightness is expected due to Doppler shift effect, such asymmetry is expected to be subtle. The observations shown here suggest that the magnitude difference is sufficiently large to be detected by Earth-based telescopes. The asymmetry is consistent in both the Northern and Southern galactic poles. The difference is also consistent across several different instruments such as DECam, SDSS, Pan-STARRS, and HST, as well as different annotation methods, that include automatic, manual, or crowdsourcing annotations through "Galaxy Zoo". The observation can also explain other anomalies such as the H_o tension. Analysis of Ia supernovae where the host galaxies rotate in the same direction relative to the Milky Way shows a much smaller tension with the H_o as estimated by the CMB.

1 Introduction

Despite over a century of research, the physics and nature of galaxy rotation is still unknown (Opik, 1922; Babcock, 1939; Oort, 1940; Rubin and Ford Jr, 1970; Rubin et al., 1978, 1980, 1985; Sofue and Rubin, 2001). Early evidence that the galaxy rotation disagree with the physical properties of galaxies were observed as early as the first half of the 20th century (Slipher, 1914; Wolf, 1914; Pease, 1918; Babcock, 1939; Mayall, 1951). In fact, the absence of Keplerian velocity decrease in the outer parts of galaxies was observed shortly after it became clear that galaxies are rotating objects (Rubin, 2000).

For instance, one of the most detailed early observations of the galaxy rotation curve anomaly was made by Jan Hendrik Oort, who analyzed the rotation and mass distribution of NGC 3115 and NGC 4494 (Oort, 1940). That work led to the conclusion that "the distribution of mass in the system appears to bear almost no relation to that of light", and that "the strongly condensed luminous system appears embedded in a large and more or less homogeneous mass of great density".

While that early work identified what is now considered the *dark matter halo*, preeminent astronomers of the time argued that the galaxy rotation was driven by Newtonian dynamics corresponding to the distribution of the visible light (De Vaucouleurs, 1959; Schwarzschild, 1954), which was based on the theory of that time. According to Rubin (2000), these opinions played a substantial role in ignoring the observations of the galaxy rotation curve anomaly, and led to adopting an incorrect Newtonian model as the physical model of galaxy rotation. Only several decades later the observations that galaxy rotation does not follow any known physical model was accepted by the "mainstream" astronomy community (Rubin, 2000).

After the tension between the galaxy rotation and its physical properties became an accepted observation, theoretical explanations were proposed. That initiated a new era in astronomy research, driven by new physical concepts that can close the gaps between theory and observations.

A notable explanation to that observation is that galaxy mass is dominated by dark matter (Zwicky, 1937) that does not interact with light or other radiation (Rubin, 1983; Bertone and Hooper, 2018). While dark matter is a theory that is currently widely accepted by the scientific community, there is still no full proof to the existence of dark matter (Sanders, 1990; Mannheim, 2006; Kroupa, 2012; Kroupa et al., 2012; Kroupa, 2015; Arun et al., 2017; Akerib et al., 2017; Bertone and Tait, 2018; Aprile et al., 2018; Skordis and Złośnik, 2019; Sivaram et al., 2020; Hofmeister and Criss, 2020). The presence of the dark matter halo in galaxies was also challenged by the profiles of their rotation curves (Byrd and Howard, 2019, 2021). The initial contention that the distribution of dark matter in the galaxy is constant (Oort, 1940; Donato et al., 2009) is in certain disagreement with its correlation with light and other galactic disk properties (Zhou et al., 2020). Research efforts towards understanding the existence and nature of the contention that the mass of galaxies is dominated by dark matter are still being continued.

Another widely discussed paradigm related to the puzzling physics of galaxy rotation is that galaxy rotation does not necessarily follow the known Newtonian Dynamics (Milgrom, 1983, 2007; De Blok and McGaugh, 1998; Sanders, 1998; Sanders and McGaugh, 2002; Swaters et al., 2010; Sanders, 2012; Iocco et al., 2015; Díaz-Saldaña et al., 2018; Falcon,

*lshamir@mtu.edu

2021). While dark matter is an important part of the standard model, the Modified Newtonian Dynamics (MOND) was also reported to be in alignment with observations (Kroupa, 2015; O'Brien et al., 2017; Wojnar et al., 2018; Milgrom, 2019). Modified gravity has also been expanded to explain other phenomena such as the acceleration of the Universe (Carroll et al., 2006). On the other hand, other studies have shown tension between MOND predictions and data (Dodelson, 2011; Zhou et al., 2020). Other explanations have also been proposed, such as (Sanders, 1990; Capozziello and De Laurentis, 2012; Chadwick et al., 2013; Farnes, 2018; Rivera, 2020; Nagao, 2020; Blake, 2021; Larin, 2022). For instance, it has been proposed that the galaxy rotation curve can be explained by models that shift from the assumption that the frame of reference of the rotational velocity is inertial (Gomel and Zimmerman, 2021). But despite substantial research in the past century, the physics of galaxy rotation is still a mystery, and currently there is not complete proven model that fully explains its puzzling nature.

1.1 Doppler shift effect on galaxy brightness

Due to the Doppler shift effect, it is expected that a galaxy that rotates in the same direction relative to the Milky Way would have different brightness compared to an identical galaxy that rotates in the opposite direction relative to the Milky Way. The brightness of a galaxy is determined by the brightness of its stars and other luminous objects, most of them are in a spin motion around the galaxy center. A star or any other light-emitting object in a galaxy rotating at velocity V_r relative to a stationary observer is expected to have a Doppler shift of its bolometric flux. The expected observed flux F of a galaxy can be calculated by Equation 1

$$F = F_o(1 + 4 \cdot \frac{V_r}{c}), \tag{1}$$

where F_o is the observed flux if the luminous object was stationary relative to the observer, and c is the speed of light (Loeb and Gaudi, 2003; Rybicki and Lightman, 2008). Assuming that $\frac{v}{c}$ is $\sim$0.0007 as is approximately the case of the Sun in the Milky Way, a star rotating in the opposite direction relative to the Milky Way and observed on the galactic pole of the Milky Way will have $\frac{v}{c}$ of 0.0014 relative to an Earth-based observer. The $\frac{F}{F_0}$ of that star as observed from the Solar system is therefore $\simeq$1.0056. The maximal expected difference between the magnitude of a face-on galaxy on the galactic pole that rotates in the same direction as the Milky Way and the magnitude of an identical galaxy spinning in the opposite direction is $-2.5 \log_{10} 1.0056 \simeq 0.006$.

When the galaxy spins, its F_o cannot be measured directly, and therefore $\frac{F}{F_o}$ cannot be determined observationally for a single galaxy. But when observing a large population of galaxies in the field centered at the galactic pole, the mean magnitude of the galaxies rotating in the same direction of the Milky Way can be compared to the mean magnitude of galaxies rotating in the opposite direction relative to the Milky Way. When a large number of galaxies is used, a statistically significant difference between the galaxy magnitude is expected. The purpose of this study is to compare the brightness of galaxies spinning in the same direction relative to the Milky Way to the brightness of galaxies that rotate in the opposite direction.

Table 1: The (α, δ) coordinates of the centered and the number of galaxies in each $60^o \times 60^o$ field.

Field center	# galaxies
$(192^o, 27^o)$	1,309,498
$(12^o, -27^o)$	6,376,803
$(102^o, 0^o)$	1,377,789
$(282^o, 0^o)$	1,266,036

The practice of applying statistical analysis using a large number of galaxies when a measurement is not possible with a single galaxy is a practice used in other tasks such as *weak lensing* (Van Waerbeke et al., 2000; Wittman et al., 2000; Mandelbaum et al., 2006; Hirata et al., 2007; Pogosian et al., 2010). Here, the expected difference of 0.006 magnitude cannot be measured for a single galaxy, and therefore is measured as the average magnitude of a population of galaxies. To observe the maximum difference of 0.006 magnitudes, all galaxies need to be pure face-on galaxies, and all of them are expected to be exactly on the galactic pole of the Milky Way. These conditions are not practical, and therefore the expected observed difference is expected to be of less then 0.006 magnitudes.

2 DECam Data

The Dark Energy Camera (DECam) is placed on the Víctor M. Blanco 4m telescope in Cerro Tololo (Flaugher et al., 2012). Its footprint covers both the Northern and Southern galactic poles, allowing to compare them using the same instrument. The DECam data used in this study is the result of nine months of continuous retrieving of the data (Shamir, 2022b), and includes the two $60^o \times 60^o$ fields centered around the Northern and Southern galactic poles. Additionally, two fields at 90^o from the galactic pole were used as control fields. The images were retrieved from the DESI Legacy Survey (Dey et al., 2019) server using the *Cutout* API. The images that were retrieved were images of objects identified as galaxies by the DESI Legacy Survey DR8 pipeline, and had magnitude lower than 19.5 in the g, r, or z filter. Each image is a 256×256 JPEG image, and the images were scaled by the Petrosian radius so that the entire galaxy fits inside the image. Because the objects are identified by the DESI Legacy Survey pipeline as extended objects, in some cases multiple objects can be part of the same galaxy. To ensure that each galaxy is represented once in the dataset, objects that have another object in the dataset within 0.01^o are excluded from the dataset. The fields and the number of galaxies imaged by DECam in each field are specified in Table 1.

The galaxies were separated by their spin directions using the *Ganalyzer* algorithm (Shamir, 2011) as described in (Shamir, 2016, 2017a, 2020c, 2017b, 2021b). Ganalyzer is a model-based method driven by defined symmetric rules. It does not make use of machine learning or other complex data-driven rules that lead to non-intuitive classification schemes, and therefore its symmetric nature can be defined. The sym-

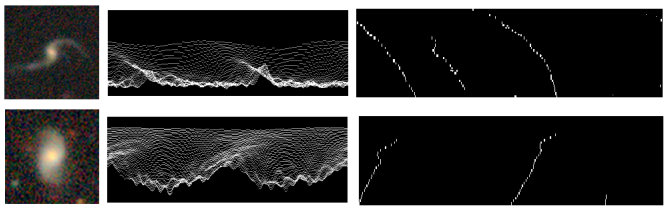

Figure 1: Examples of original images (left), the radial intensity plots (center), and the peaks identified in the lines of the radial intensity plots (right). The direction of the lines generated by the peaks determines the direction of the galaxy arms.

metricity of the algorithm ensures that the algorithm is not systematically biased, which is far more difficult to verify when using algorithms based on complex non-intuitive rules as typical in approaches such as deep neural networks.

In summary, the algorithm works by first converting each galaxy image into its radial intensity plot. The radial intensity plot of a galaxy image is a 35×360 image, in which the value of the pixel at image coordinates (x, y) is the median of the values of the 5×5 pixels around pixel coordinates $(O_x + \sin(\theta) \cdot r, O_y - \cos(\theta) \cdot r)$ in the galaxy image, where r is the radial distance in percentage of the galaxy radius, (O_x, O_y) is the center of the galaxy, and θ is the polar angle measured in degrees from the galaxy center.

In spiral galaxies the arms are brighter than the background, and therefore pixels on the galaxy arms are expected to be brighter than the pixels at the same radial distance that are not on the arm. Therefore, the peaks in the radial intensity plot are expected to correspond to pixels on the galaxy arms. The arms can therefore be identified by applying a peak detection algorithm (Morháč et al., 2000) to the different lines in the radial intensity plot. After the peaks are identified, a linear regression is applied to the peaks in neighboring lines. The sign of the slope of the lines formed by the peaks reflects the direction of the curves of the arms, and consequently the spin direction of the galaxy (Shamir, 2016, 2017a, 2020c, 2017b, 2021b). Figure 1 shows an example of galaxy images, the radial intensity plots rendered from each galaxy image, and the peaks identified in the radial intensity plots.

Many galaxies are elliptical, and their spin directions cannot be determined. Other galaxies might not be elliptical, but still do not have identifiable direction of their spin. Since the spin directions of some galaxies cannot be determined, it is required to remove such galaxies from the analysis. That was done by selecting only galaxies that the number of peaks in their radial intensity plot (as shown in Figure 1) that shift in one direction is at least three times larger than the number of peaks that shift towards the opposite direction. Also, galaxies that had less than 30 peaks in their radial intensity plot were also not used in the analysis, as was done in (Shamir, 2016, 2017a,b, 2020c, 2021a,b). The full description of the Ganalyzer algorithm is available in (Shamir, 2011; Dojcsak and Shamir, 2014; Shamir, 2016, 2017a,b, 2020c, 2021b).

The simple "mechanical" nature of *Ganalyzer* ensures that it is symmetric, as was also tested empirically in several previous studies. For instance, Figure 5 and Figure 9 in (Shamir, 2022c) show the results of the annotation after mirroring the galaxy images. A certain downside of using such analysis is that the annotation is not complete in the sense that all galaxies that have an identifiable spin direction are indeed annotated. Figure 2 shows an example of galaxies imaged by DECam, and the same galaxies imaged by Hubble Space Telescope (HST). As the figure shows, galaxies that have clear spin direction would be annotated as galaxies that do not have an identifiable spin direction, and therefore rejected from the analysis. Clearly, using HST images will also be subjected to incompleteness, as HST has its own limits on its imaging power. Since no telescope can provide a complete dataset in which the spin directions of all galaxies can be identified, the importance of the algorithm is its symmetric nature.

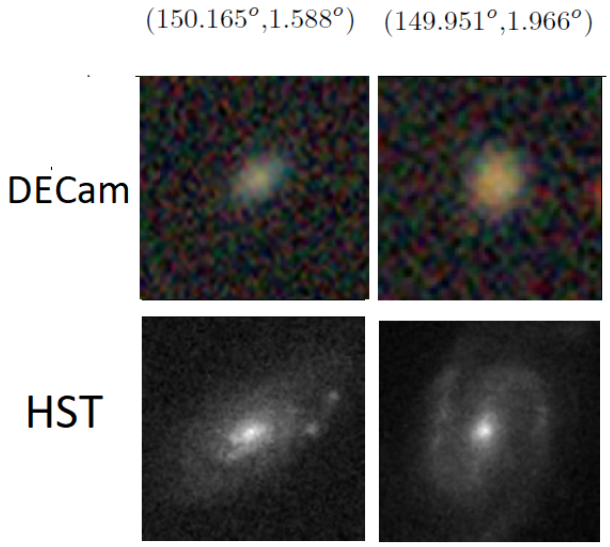

Figure 2: Galaxies imaged by DECam and the same galaxies imaged by Hubble Space Telescope. The spin direction is clear in the HST images, but not clear in the DECam images.

After separating the galaxy images by their spin directions, 400 random galaxies were observed, and none of these galaxies had a spin direction opposite to the spin direction it was annotated by the algorithm. While that does not ensure that the entire dataset does not have any wrongly annotated galaxies, it can be safely assumed that the dataset was into two subsets such that the first subset has a much higher frequency of galaxies that spin clockwise, and the second subset has a much higher frequency of galaxies that rotate counterclockwise. Another subset includes galaxies that their spin direction could not be determined, but due to the symmetric nature of the algorithm that subset is not expected to affect the ratio between the other two subsets. As will be shown in Section 3, the inverse results in the opposite sides of the Galactic pole show no consistent bias of the algorithm.

3 Results of DECam data

Tables 2 and 3 show the difference between the mean magnitude of galaxies spinning in opposite ways in the fields around the North and the South galactic pole, respectively. To avoid potential erroneous magnitude values that can skew the mean

magnitude, all magnitude values lower than 10 or greater than 25 were rejected from the analysis. The bands that were used in this study are the three optical bands of DESI Legacy Survey, which are the g, r, and z bands. Some galaxies do not have values for the flux in all bands, and that leads to a slightly different number of galaxies used in each band.

The tables show the differences in the mean brightness between galaxies that spin in opposite directions at the field around the galactic poles. The tables show that the differences are statistically significant, as determined by the one-tailed P values of the Student t-test (Helmert, 1876). While the differences in magnitude are observed in both hemispheres, the direction of the difference is inverse, such that clockwise galaxies are brighter in one hemisphere but dimmer in the opposite hemisphere.

The inverse difference in magnitude agrees with the expected difference caused by relativistic beaming in the two opposite sides of the galactic pole. It also shows that it is not caused by a bias of the annotation algorithm of photometric pipeline, as such bias is expected to be consistent across different fields, and is not expected to flip between the North and South galactic poles. When dividing the galaxies into two random groups, regardless of their spin direction, the asymmetry becomes statistically insignificant. For instance, the G magnitude becomes 20.08321±0.010 and 20.08318±0.010.

Tables 2 and 3 also show differences in the number of galaxies that rotate clockwise compared to the number of galaxies that rotate counterclockwise. These differences difference agree with the magnitude difference, as it is expected that if one type of galaxies is brighter to an Earth-based observer than the other type, more galaxies of that type will be identified. Previous reports on the large-scale differences between the number of galaxies spinning in opposite directions can be found in (Shamir, 2020c, 2022b,d,c), and their link to brightness differences is discussed in (Shamir, 2020a, 2017a, 2022a). The brightness of galaxies also correlates with their shape (Kormendy, 1977), and the correlation was also observed (Shamir, 2022e). In summary, if one type of galaxies is indeed brighter to an Earth-based observer, the observed difference in the number of galaxies spinning in opposite directions can be the result of the difference in magnitude rather than the real population of spiral galaxies in the Universe.

The difference between the mean magnitude of galaxies spinning in opposite directions around the fields of the Northern and Southern galactic poles was compared to the two control fields that were selected as fields that are 90^o away from the galactic pole. Tables 4 and 5 show the difference in magnitude around these fields. The tables use 47,017 and 41,244 galaxies, respectively. As both tables show, there is no statistically significant magnitude difference between the galaxies in these two fields. That shows that in 90^o from the galactic pole, there is no observed difference between the brightness of galaxies spinning in opposite ways, as is the case for galaxies at around the galactic pole. That can be viewed as a link between the galactic pole and the differences in the brightness of galaxies spinning in opposite directions.

4 Experiment with SDSS galaxies

DECam provides images of a large number of galaxies, but until the Dark Energy Spectroscopic Instrument (DESI) sees first light most of these galaxies do not have spectra. To test a set of galaxies with spectra we used SDSS data. SDSS is inferior to DECam in its imaging capabilities, but as a mature redshift survey it collected spectra for a relatively high number of galaxies.

Images of 666,416 galaxies were downloaded by using the SDSS *cutout* API. The initial file format was 128×128 JPEG, and each file was converted to the PNG format. These images were annotated by the *SpArcFiRe* (Scalable Automated Detection of Spiral Galaxy Arm) algorithm (Davis and Hayes, 2014; Hayes et al., 2017). To test for consistency, the galaxy images were also mirrored by using the "flip" command of *ImageMagick*. That led to two annotated datasets, the first is the annotations of the original images, and the other is the annotations of the mirrored images. *SpArcFiRe* is an open source software with available source code[1]. *SpArcFiRe* is described in detail in (Davis and Hayes, 2014). The method works by identifying arm segments, and can then fit these segments to a logarithmic spiral arc. That allows *SpArcFiRe* to determine the spin direction of the galaxy. *SpArcFiRe* is a model-driven method, and is not based on machine learning that can lead to biases that are very difficult to detect (Dhar and Shamir, 2022).

The disadvantage of *SpArcFiRe* is that it has a certain error in the annotation, as also noted in Appendix A in (Hayes et al., 2017). The *Ganalyzer* algorithm described in Section 2 allows to adjust the accuracy of the annotation by setting the minimum number of peaks required to make an annotation. If the number of peaks identified in the radial intensity plot is lower than the threshold, the galaxy is not used in the analysis. That leads to the rejection of a large number of galaxies. In the case of DECam, the initial number of galaxies is very high, and therefore even after rejecting a large number of galaxies the remaining galaxies make it a sufficiently large dataset to allow statistical analysis. *SpArcFiRe*, on the other hand, is far slower and has a certain error, but it also rejects a smaller number of galaxies. The use of *SpArcFiRe* also allows to use two different analysis methods.

Classification of a single 128×128 galaxy image requires ∼30 seconds when using a single core of a recent Intel Core-i7 processor. To reduce the response time, 100 cores were used to annotate the image data using *SpArcFiRe*. Figure 3 displays the RA distribution of the galaxies. As the figure shows, the galaxy population is not distributed uniformly in the sky.

As the figure shows, the distribution of SDSS galaxies in the sky is not uniform. Fortunately for this specific study, the population of SDSS galaxies is relatively dense around the Northern galactic pole. That allows to study the difference in brightness of galaxies that spin with or against the spin direction of the Milky Way.

The annotation provided 271,063 galaxies annotated by their spin directions. *SpArcFiRe* was then applied again to the mirrored images, providing a set of 271,308 annotated galaxies. The slight difference between the results of the orig-

[1] https://github.com/waynebhayes/SpArcFiRe

Table 2: The g, r, and z magnitude and the number of clockwise and counterclockwise galaxies in the $60^o \times 60^o$ field centered around the North galactic pole ($\alpha = 192^o, \delta = 27^o$).

Band	# cw galaxies	# ccw galaxies	Mag ccw	Mag cw	ΔMag	t-test P
G	20,918	21,253	20.06525±0.010	20.10073±0.010	-0.03548	0.01
R	20,917	21,251	18.98522±0.008	19.01481±0.008	-0.02958	0.01
Z	20,925	21,261	18.2934±0.007	18.31783±0.007	-0.02443	0.01

Table 3: The magnitude and number of clockwise and counterclockwise galaxies in the field centered around the South galactic pole ($\alpha = 12^o, \delta = -27^o$).

Band	# cw galaxies	# ccw galaxies	Mean Mag ccw	Mean Mag cw	ΔMag	t-test P
G	87,640	89,534	20.13622±0.004	20.11937±0.004	0.01685	0.003
R	87,917	89,849	19.08793±0.003	19.07216±0.003	0.01574	0.0002
Z	88,228	90,142	18.38424±0.003	18.37225±0.003	0.01199	0.0047

Table 4: The average magnitude of galaxies that rotate clockwise and galaxies that rotate counterclockwise in the $60^o \times 60^o$ window centered around the control field of ($\alpha = 102^o, \delta = 0^o$).

Band	Mag ccw	Mag cw	ΔMag	P
G	20.16695±0.009	20.16628±0.009	0.000669	0.96
R	19.09924±0.007	19.10284±0.007	-0.00356	0.713
Z	18.39402±0.006	18.39436±0.006	-0.00032	0.972

Table 5: The mean magnitude of clockwise and counterclockwise galaxies in the $60^o \times 60^o$ window centered around the control field of ($\alpha = 282^o, \delta = 0^o$).

Band	Mag ccw	Mag cw	ΔMag	P
G	20.21329±0.01	20.22103±0.01	-0.00774	0.58
R	19.0787±0.008	19.0869±0.008	-0.0082	0.47
Z	18.37519±0.007	18.37565±0.007	-0.00045	0.96

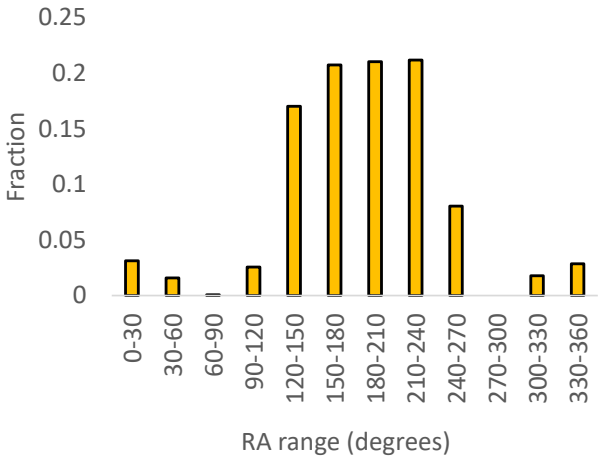

Figure 3: The RA distribution of the SDSS galaxies.

Band	Mag cw	Mag ccw	ΔMag	P t-test
G	17.7652±0.004	17.7558±0.004	0.0094	0.035
R	17.0016±0.003	16.9922±0.003	0.0094	0.013
Z	16.449±0.003	16.4357±0.003	0.0132	0.001

Table 6: The g, r, and z exponential magnitudes of SDSS galaxies that spin with the Milky Way and galaxies that spin in the opposite direction compared to the Milky Way in the field centered around the North galactic pole.

inal images and the mirrored images is discussed in (Hayes et al., 2017), and will also be discussed later in this paper.

A first experiment was by just applying *SpArcFiRe* without any first step of selecting spiral galaxies. While the annotation of galaxies that are not spiral can add noise, it might be expected that the error in the annotation will be distributed evenly between galaxies that spin clockwise and galaxies that spin counterclockwise. The *SpArcFiRe* method does not force a certain spin direction for every galaxy, and can annotate galaxies as not rotating in any identifiable direction. When *SpArcFiRe* is not able to identify the spin direction of the galaxy, that galaxy is ignored, and not used in the analysis. Table 6 shows the magnitude differences in the field of $60^o \times 60^o$ around the Northern galactic pole. The annotation process provided 55,223 galaxies spinning counterclockwise, and 55,051 spinning clockwise in that field. Because *SpArcFiRe* is not fully symmetric, the experiment was repeated after mirroring all galaxy images, and the results are shown in Table 7. The annotation of the mirrored images provided a dataset of 55,874 mirrored galaxies spinning clockwise and 54,488 mirrored galaxies spinning counterclockwise. The coordinates of the galaxies and their *SpArcFiRe* annotations are at `https://people.cs.ksu.edu/~lshamir/data/sparcfire`.

As the tables show, despite the certain inaccuracy of *SpArcFiRe*, the analysis still shows differences in the brightness of galaxies that rotate clockwise and galaxies that rotate counterclockwise in the field centered at the galactic pole. As expected, mirroring the galaxy images showed inverse results.

SpArcFiRe is designed to analyze spiral galaxies (Hayes

Band	Mag cw	Mag ccw	ΔMag	P t-test
G	17.7576±0.004	17.762±0.004	-0.0044	0.21
R	16.9936±0.003	17.0016±0.003	-0.008	0.025
Z	16.4357±0.003	16.4479±0.003	-0.0122	0.002

Table 7: The g, r, and z exponential magnitudes of mirrored SDSS galaxies that spin with the Milky Way and galaxies that spin in the opposite direction compared to the Milky Way in the field centered around the North galactic pole.

Band	Mag cw	Mag ccw	ΔMag	P t-test
G	17.7095±0.005	17.6948±0.005	0.0147	0.0376
R	16.9893±0.004	16.9745±0.004	0.0148	0.0089
Z	16.4564±0.004	16.4393±0.004	0.0171	0.0025

Table 8: The g, r, and z exponential magnitudes of SDSS galaxies annotated as spiral galaxies. The analysis is limited to galaxies in the $60^o \times 60^o$ centered at the Northern galactic pole.

et al., 2017). To apply *SpArcFiRe* to spiral galaxies, a set of spiral galaxies was separated from the other galaxies by using the *Ganalyzer* method (Shamir, 2011). In addition to its ability to identify the spin direction of galaxies, *Ganalyzer* can also separate spiral galaxies from elliptical galaxies. As a model-based method, the analysis does not involve any kind of machine learning, deep learning, or any other form of pattern recognition, and therefore it is not subjected to possible biases in the training data or the learning process (Dhar and Shamir, 2022). The simple "mechanical" nature of *Ganalyzer* allows it to be fully symmetric (Shamir, 2021b, 2022c).

Table 8 shows the number of clockwise and counterclockwise galaxies in the SDSS data after selecting the spiral galaxies, limited to the $60^o \times 60^o$ part of the sky centered at the Northern galactic pole. That dataset contained 27,196 galaxies spinning clockwise and 27,671 galaxies spinning counterclockwise. Since SDSS footprint covers mostly the Northern hemisphere, the Southern galactic pole is outside of its footprint. According to Table 8, the results show statistically significant differences between the brightness of galaxies that spin in opposite directions.

The SDSS galaxies used in this study have redshift, which allows to separate them to redshift ranges. Table 9 shows the same analysis, but when limiting the galaxies to $z < 0.07$. When limiting the redshift to 0.07, the dataset included 8,409 clockwise galaxies and 8,748 counterclockwise galaxies. The results show a larger difference in magnitude in that redshift range. That, however, is not necessarily of an astronomical meaning, and could be linked to the better ability of *SpArcFiRe* to annotate galaxies at lower redshift ranges. As the other experiments with SDSS galaxies, the results are in agreement with the results of the DECam galaxies shown in Section 3.

Band	Mag cw	Mag ccw	ΔMag	P t-test
G	16.9437±0.009	16.9192±0.009	0.0245	0.027
R	16.4017±0.009	16.3723±0.009	0.0294	0.01
Z	15.9827±0.009	15.9499±0.009	0.0328	0.005

Table 9: The g, r, and z magnitudes of SDSS galaxies limited to $z < 0.07$ that spin in the opposite directions in the field centered around the North galactic pole.

Table 10: The g, r, and z exponential magnitudes of SDSS galaxies that spin in the opposite directions in 60×60 degree window centered at the Northern galactic pole.

Band	Mag cw	Mag ccw	ΔMag	P t-test
G	17.3834±0.017	17.3382±0.017	0.0452	0.03
R	16.8389 ±0.017	16.7934±0.017	0.0455	0.029
Z	16.4071±0.018	16.3597±0.018	0.0474	0.0245

4.1 Experiment with SDSS data annotated by Ganalyzer

Since *SpArcFiRe* has a small asymmetry (Hayes et al., 2017), another experiment was done by applying the *ganalyzer* algorithm described in Section 2 to SDSS DR7 galaxies with spectra. As explained in Section 2, *Ganalyzer* rejects galaxies it cannot determine their spin direction, resulting in a smaller dataset compared to *SpArcFiRe*. On the other hand, it provides a symmetric and consistent dataset that is not expected to be biased. The dataset is available at `https://people.cs.ksu.edu/~lshamir/data/sdss_phot/`. The dataset contains 6,103 galaxies such that 3,058 galaxies spin clockwise, and 3,045 galaxies spin counterclockwise.

Table 10 shows the g, r, and z exponential magnitudes for galaxies that spin clockwise and counterclockwise in the 60×60 degree field centered at the Northern galactic pole. As in the other experiments, the table shows statistically significant magnitude differences between the average brightness of the galaxies.

4.2 Analysis with crowdsourcing data from *Galaxy Zoo 1*

One of the previous attempts to annotate galaxies by their spin direction was done by crowdsourcing through the *Galaxy Zoo 1* project (Lintott et al., 2008). According to Galaxy Zoo 1, anonymous volunteers used a web-based user interface to manually annotate galaxies by their shape. Among other features, the users were asked to annotate the spin direction of the galaxies. While not all annotations are expected to be correct, the majority of the votes is expected to provide a certain indication regarding the spin direction.

The Galaxy Zoo annotations can be used to perform an experiment similar to the experiments described above, but with galaxies annotated manually by a large number of volunteers. Fortunately, the $60^o \times 60^o$ part of the sky centered around the Northern galactic pole is fairly populated by galaxies that were annotated through Galaxy Zoo 1, and the majority of Galaxy Zoo annotated galaxies are concentrated around that

Band	Mag cw	Mag ccw	ΔMag	P t-test
G	16.9765±0.01	16.9579±0.01	0.0186	0.09
R	16.4129±0.01	16.3723±0.01	0.0406	0.002
Z	15.9817±0.01	15.9539±0.01	0.0278	0.025

Table 11: The g, r, and z exponential magnitudes of SDSS galaxies annotated by Galaxy Zoo in the field centered around the North galactic pole.

Band	Mag cw	Mag ccw	ΔMag	P t-test
G	16.3496±0.03	16.3122±0.03	0.0374	0.189
R	15.7912±0.03	15.7443±0.03	0.0468	0.135
Z	15.377±0.03	15.3235±0.03	0.0535	0.104

Table 12: The g, r, and z magnitudes of SDSS galaxies annotated as "superclean" by Galaxy Zoo in the field centered around the North galactic pole.

part of the sky. That allows to obtain the profile of brightness differences between galaxies that were annotated by Galaxy Zoo to spin clockwise, compared to the brightness of Galaxy Zoo galaxies that were annotated as spinning counterclockwise.

The Galaxy Zoo 1 annotations were taken from the "zooVotes" table of SDSS DR8. The galaxies include only galaxies of which 60% or more of the voters agreed on their spiral nature and spin direction. That is, the field "p_cw" was greater or equal to 0.6 for galaxies that spin clockwise, and the field "p_acw" was greater or equal to 0.6 for galaxies that spin counterclockwise. As before, missing values or flag values were removed. That provided a dataset of 11,150 galaxies spinning clockwise, and 11,907 galaxies spinning counterclockwise. All galaxies are inside the $60^o \times 60^o$ region centered at the Northern galactic pole. Table 11 shows the brightness differences in the g, r, and z bands for the Galaxy Zoo galaxies. As the table shows, the differences between the brightness of galaxies spinning in opposite directions in the Northern galactic pole are noticeable also in the galaxies annotated by Galaxy Zoo. The corresponding part of the sky in the Southern galactic pole has merely a total of 2,005 annotated galaxies, and therefore analysis of the Southern galactic pole is not possible in the same manner it was done with the DECam data.

The *Galaxy Zoo 1* defines a "superclean" annotation as an annotation that 95% of the annotators provided the same annotation. Table 12 shows the differences in brightness of galaxies in the $60^o \times 60^o$ region around the Northern galactic pole such that all annotations of the galaxies meet the "superclean" criterion. The requirement for higher agreement of the annotators can lead to cleaner annotations, but that comes on the expense of the size of the dataset. When using just galaxies on which 95% of the annotators agree, the total number of annotated galaxies is merely 4,065. The number of clockwise galaxies is 1875, and the number of galaxies annotated as spinning counterclockwise is 2190. The results also show that galaxies spinning counterclockwise around the North galactic pole are brighter. The results are not statistically significant, which can be attributed to the smaller number if galaxies that satisfy the higher annotation agreement threshold. But the difference observed in the "superclean" galaxies also does not conflict with the difference observed with the larger datasets.

The Galaxy Zoo annotations are known to be subjected to certain biases that are often difficult to fully profile (Hayes et al., 2017). The brightness differences observed with galaxies annotated by Galaxy Zoo can therefore be the result of some unknown bias where the volunteers tend to annotate brighter galaxies as galaxies rotating counterclockwise. These biases can be difficult to quantify and fully profile, and therefore the results when using the Galaxy Zoo annotations might not be sufficient to provide strong evidence of brightness differences. The agreement between the results of Galaxy Zoo and the results of DECam and SDSS can also be considered a coincidence. But the results of Galaxy Zoo also do not conflict with the results shown with the automatically annotated galaxies, and in fact are in good agreement with the other experiments. Whether the agreement is the result of an astronomical reason or a certain unidentified human bias is still a matter that is difficult to fully determine due to the complex nature of the possible human biases of the crowdsourcing-based annotations.

Band	Mag cw	Mag ccw	T-test P
G	16.9066±0.02	16.9972±0.02	0.0014
R	16.3463±0.02	16.4226±0.02	0.007
Z	15.8408±0.02	15.9087±0.02	0.0164

Table 13: The g, r, and z exponential magnitudes of Pan-STARRS galaxies at around the Southern galactic pole.

5 Analysis with Pan-STARRS data

A sky survey that covers more of the Southern sky than SDSS is Pan-STARRS. Like SDSS, Pan-STARRS covers mostly the Northern sky, but its footprint covers more of the Southern hemisphere compared to SDSS. Using a dataset of Pan-STARRS DR1 galaxies used in a previous study (Shamir, 2017a) provided the magnitude difference of 3,587 galaxies in the $60^o \times 60^o$ around the Southern galactic pole. The galaxies can be accessed at `https://people.cs.ksu.edu/~lshamir/data/assym3/`. The results show that in the part of the sky around the Southern galactic pole galaxies that spin clockwise are brighter than galaxies that spin counterclockwise. That difference is in agreement with the results of DECam for the Southern galactic pole. The results are shown in Table 13.

6 HST data

As ground-based instruments, DECam, SDSS, and Pan-STARRS are subjected to the effect of the atmosphere. There is no known atmospheric effect that can affect galaxies differently based on their spin direction, and therefore the atmosphere is not expected to lead to such difference. To test empirically whether the difference is consistent also when imaging the galaxies without the effect of the atmosphere, we used galaxies imaged by the Hubble Space Telescope (HST). These results were shown initially in (Shamir, 2020a).

The galaxies used in this experiment were imaged by the Cosmic Evolution Survey (COSMOS) of HST. As the largest HST field, COSMOS (Scoville et al., 2007; Koekemoer et al., 2007; Capak et al., 2007) covers ∼2 square degrees, centered at ($\alpha = 150.119^o$, $\delta = 2.2058^o$). The initial list of objects included 114,630 COSMOS objects that are at least 5σ brighter than their background. Each galaxy image was separated from the F814W image by using the *Montage* (Berriman et al., 2004) tool. The images were annotated by the Ganalyzer algorithm (Shamir, 2011), and then inspected manually. That led to a dataset of 2,607 galaxies that rotate clockwise, and 2,515 galaxies that rotate counterclockwise. Full details of the annotation process are provided in (Shamir, 2020a), and the data is available at `http://people.cs.ksu.edu/~lshamir/data/assym_COSMOS/`.

Table 14 shows the brightness in the g, r, and z filters of galaxies spinning in opposite directions. The magnitudes are the Subaru AB magnitudes (Capak et al., 2007). The comparison provides certain evidence that in the COSMOS field galaxies that spin counterclockwise are brighter than galaxies that spin clockwise. The COSMOS field is not aligned with neither the Northern nor the Southern galactic pole, but it is far closer to the Northern galactic pole. According to the other experiments described earlier in this paper, in the Northern galactic pole galaxies that spin counterclockwise are expected to be brighter. That observation is aligned with the results observed with the HST galaxies, reported in (Shamir, 2020a). The difference in the z band is not necessarily statistically significant, but the findings are aligned with the results shown by the other telescopes, and definitely do not conflict with DECam, SDSS and Pan-STARRS.

Band	Mag cw	Mag ccw	ΔMag	P (t-test)
G	23.131±0.019	23.077±0.019	0.054	0.023
R	22.266±0.019	22.218±0.02	0.048	0.045
Z	21.358±0.017	21.323±0.018	0.035	0.087

Table 14: The brightness of HST galaxies spinning in opposite directions in the COSMOS field.

7 Non-astronomical reasons that can lead to differences in brightness

The differences in brightness between galaxies spinning in opposite directions cannot be determined by direct observation, but by analysis of a large number of galaxies. Large-scale analysis of a high number of galaxies to determine properties that are difficult to obtain with direct measurements is not a new practice, and is used in tasks such as weak gravitational lensing (Van Waerbeke et al., 2000; Wittman et al., 2000; Mandelbaum et al., 2006; Hirata et al., 2007; Abbott et al., 2016). The purpose of this section is to review the analysis and possible errors that can lead to the observation.

7.1 Incorrectly annotated galaxies

One of the key aspects of the analysis shown here is the annotation of the galaxies by their spin direction. Two different algorithms were used in this study, as well as manually annotated galaxies using crowdsourcing, all show similar results. For the computer-based annotations, the experiments were repeated after mirroring the galaxy images, leading to inverse results. Also, the brightness difference is inverse in the Northern galactic pole compared to the Southern galactic pole. A bias in the algorithm is expected to be consistent in both ends of the Galactic pole, rather than flip.

Also, if an algorithm that annotates the galaxies by their spin directions annotates some of the galaxies with wrong spin direction, the real brightness difference ΔM at a certain part of the sky is determined by Equation 2

$$\Delta M = ((1-e)\bar{M_{cw}} + e\bar{E_{cw}}) - ((1-e)\bar{M_{ccw}} + e\bar{E_{ccw}}), \quad (2)$$

where $\bar{M_{cw}}$ is the mean magnitude of galaxies spinning clockwise that are also annotated correctly by the classifier as galaxies spinning clockwise, $\bar{M_{ccw}}$ is the mean magnitude of galaxies spinning counterclockwise that are also annotated correctly as spinning counterclockwise, $\bar{E_{cw}}$ is the mean magnitude of galaxies spinning counterclockwise but annotated incorrectly as spinning clockwise. $\bar{E_{ccw}}$ is the mean magnitude of galaxies spinning clockwise but were annotated incorrectly as spinning counterclockwise, and e is the error rate of the annotation algorithm. The equation can be re-written as

$$\Delta M = \bar{M_{cw}} - \bar{M_{ccw}} + e(\bar{E_{cw}} - \bar{E_{ccw}} + \bar{M_{ccw}} - \bar{M_{cw}}). \quad (3)$$

Let $\vartheta = \bar{M_{cw}} - \bar{M_{ccw}}$ and $\varphi = \bar{E_{cw}} - \bar{E_{ccw}}$. ΔM can be now expressed as $\Delta M = \vartheta + e(\vartheta - \varphi)$. If the magnitude between clockwise and counterclockwise galaxies is different, it should be consistent for all galaxies, including galaxies that are annotated incorrectly. In that case, $\varphi = -\vartheta$, and $\Delta M = \vartheta + e(2\vartheta)$. Because $e \geq 0$, the real magnitude difference ΔM can only be larger than ϑ, and can only becomes larger when the error of the annotation algorithm e grows. That shows that if there is a certain error in the annotation algorithm, the real magnitude difference will be larger than the observed magnitude difference.

7.2 Cosmic variance

Galaxies as observed from Earth are not distributed in the sky in a fully uniform manner, leading to subtle fluctuations in galaxy density known as "cosmic variance" (Driver and Robotham, 2010; Moster et al., 2011). These small fluctuations in galaxy population density can affect measurements at different parts of the sky and different directions of observation (Kamionkowski and Loeb, 1997; Camarena and Marra, 2018; Keenan et al., 2020).

The probe used in this study is the brightness difference between galaxies imaged in the same part of the sky, by the same telescope, in the same exposure, and the same analysis methods. That is, anything that might affect the brightness of galaxies that spin with the Milky Way is also expected to affect galaxies spinning in the opposite direction. There is no attempt to compare magnitudes measured in two different parts of the sky, two different instruments, or even two different exposures. In all experiments the mean brightness of

galaxies spinning in one direction is compared to the mean brightness of galaxies spinning in the opposite way such that all galaxies are in the exact same part of the sky. Any cosmic variance that might affect galaxies spinning with the Milky Way is expected to affect the mean magnitude of galaxies spinning in the opposite direction.

7.3 Bias in the hardware or photometric pipelines of digital sky surveys

Digital sky surveys are some of the more complex research instruments of our time. That complexity makes it very difficult to inspect every single part of these systems and ensure that no bias exists. At the same time, it is also difficult to propose a certain possible flaw that can lead to differences in the brightness of galaxies that spin in the same direction as the Milky Way and galaxies that spin in the opposite direction. Moreover, the difference in brightness flips between the Northern and Southern galactic poles, making it more difficult to propose an explanation based on a possible hardware or software flaw.

In this study, several different digital sky surveys were used, and the results are consistent across the different telescopes. While it is challenging to propose of a specific flaw in a digital sky survey that exhibits itself in such form in a single telescope, it is more difficult to think of such flaw in several unrelated sky surveys.

7.4 Atmospheric effect

Atmospheric effect might change the brightness of galaxies as observed from Earth, and can lead to differences in brightness observed in different parts of the sky. As also discussed in 7.2, the comparison between the magnitudes are done in the same part of the sky, and all galaxies were taken from the exact same frames and exposures. Therefore, all atmospheric effects that can change the magnitude of galaxies that spin in one direction are expected to change the magnitude of galaxies that spin in the opposite direction.

To completely eliminate the atmospheric effect, an experiment was done with data from Hubble Space Telescope. That experiment is described in Section 6. The results of that experiment are consistent with the results from the ground-based telescopes, providing another indication that the difference in brightness is not the result of the effect of the Earth's atmosphere.

7.5 Spiral galaxies with leading arms

Although the vast majority of spiral galaxies have trailing arms, in some less common cases a spiral galaxy can have leading arms. For instance, a notable example of a galaxy with leading spirals arms is NGC 4622 (Freeman et al., 1991; Buta et al., 2003; Byrd et al., 2007). Assuming that the spin direction of a galaxy is driven by the perspective of the observer, the frequency of galaxies with leading arms among galaxies that spin in the same direction as the Milky Way is similar to the frequency of galaxies spinning in the opposite direction. In that case, galaxies with leading arms can be considered as galaxies that were annotated incorrectly, and subjected to the same analysis shown in Section 7.1.

8 Possible link to H_o tension

The purpose of this section is to show a link between the observation reported in the previous sections and the H_o tension, and provide a possible solution to the tension that does not require changing the standard cosmological model (Shamir, 2023). The Hubble-Lemaitre constant (H_o) tension (Wu and Huterer, 2017; Mörtsell and Dhawan, 2018; Bolejko, 2018; Davis et al., 2019; Pandey et al., 2020; Camarena and Marra, 2020; Di Valentino et al., 2021c; Riess et al., 2022) is one of the most puzzling cosmological observations, and currently has no proven explanation. The observation is difficult to explain by modification of gravity (Pogosian et al., 2022), and challenges the validity of the standard cosmological model (Di Valentino et al., 2021a,b). In summary, the Hubble-Lemaitre constant H_o determined by using Ia supernovae or Cepheids to measure the distance of galaxies is different from the constant measured with other probes such as the CMB radiation. Since the different probes measure the same Universe, one of the explanations to the tension is that one or more of these probes have slight inaccuracies that lead to the different H_o values. For instance, it has been suggested that Lorentz Relativistic Mass can affect the measurements using Ia supernovae (Haug, 2022). The effect of dust on Ia supernovae distant measurement has also been proposed (Brout and Daniel, 2020).

The Hubble-Lemaitre constant can be determined by using probes such as Cepheids or Ia supernovae to measure distances at cosmological scales, and these distances are compared to the velocity of galaxies by using their redshift. Ia supernovae and Cepheids have expected absolute magnitudes, and therefore their apparent magnitude as observed from Earth can be used to determine the distance of their host galaxy from Earth.

Supernovae are explosions of stars, and therefore their rotational velocity is inherited from the star they were created from. Cepheids are also stars, and therefore also have the rotational velocities of their host galaxies. The magnitude of the Ia supernova is measured from Earth, which has the rotational velocity of the Milky Way galaxy at around 220 km $\cdot$ sec $^{-1}$. If the rotation of the galaxies that host Ia supernovae compared to the rotation of the Milky Way can affect the apparent magnitude of the supernova, that can lead to a different distance metrics that depends on the rotation of the host galaxy of the Ia supernova compared to the rotation of the Milky Way. That is, because not all supernovae used in the measurements are located around the galactic pole and spin in the same direction as the Milky Way, their apparent magnitude might seem slightly different to an Earth based observer, leading to a slight change in their estimated distance, and consequently to the measured Hubble-Lemaitre constant. Because the rotational velocity of a galaxy correlates with the galaxy type, the link between rotational velocity and H_o can be related to previous reports on correlation between H_o and the type of the Ia supernova host galaxy (Khetan et al., 2021). Other studies also suggested a link between Ia supernova and the properties of its host galaxies (Meldorf et al., 2022; Dixon

Rotation direction	#	H_o	3% error range	SD
All	96	73.758	70.193-77.404	1.943
Same direction	22	69.049	62.955-76.005	3.42
Opposite direction	36	74.182	68.758-79.915	3.2

Table 15: The H_o determined when using the full set, the H_o determined when using a subset such that the host galaxies rotate in the same direction relative to the Milky Way, and the H_o determined when using a subset such that the host galaxies rotate in the opposite direction.

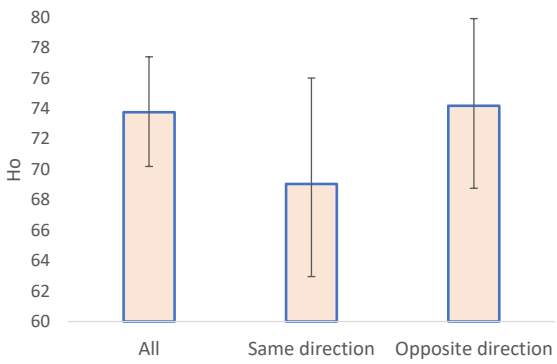

Figure 4: The H_o computed when using the entire set, and when limiting the dataset to supernovae in galaxies rotating in the same direction relative to the Milky Way, and to supernovae in galaxies rotating in the opposite direction relative to the Milky Way. The error bars are the 3% errors. Due to the relatively small number of data points, this experiment does not necessarily provide a proof, and analysis with more data will be needed. But these results are in agreement with the observations according which the rotational velocity relative to the Milky Way can affect the apparent brightness of objects.

et al., 2022).

An experiment that would test that assumption can be made by computing the Hubble-Lemaitre constant by using only host galaxies that rotate in the same direction as the Milky Way. Such galaxies can be from both the Northern and Southern hemispheres. If the measurement of the Hubble-Lemaitre constant when using host galaxies that rotate with the Milky Way provides a different result than when using all galaxies, that can provide an indication that the spin direction affects the determined Hubble-Lemaitre constant. If the result is also close to the Hubble-Lemaitre constant as determined by the CMB radiation, that can also explain the H_o tension, and might also explain other observation made with Ia supernovae as distance candles.

To perform a simple test, we used the code and data provided by Khetan et al. (2021) for determining the H_o constant. Khetan et al. (2021) use a set of 140 Ia supernovae, and two calibration sets. The *SH0ES* calibration uses 19 Cepheids. The full description of the data and calibration is provided in (Khetan et al., 2021).

In addition to using the 140 supernovae as done in (Khetan et al., 2021), we also separated a subset of the 140 supernovae into supernovae within 60^o from the Northern galactic pole and their host galaxies spin clockwise, or within 60^o from the Southern galactic pole and their host galaxies spin counterclockwise. That provided a set of 34 supernovae that rotate at the same direction as the Milky Way, and 48 supernovae that rotate in the opposite direction. As done in (Khetan et al., 2021), galaxies with redshift lower than 0.02 were removed, reducing the sets to 22 and 36 supernovae, respectively. Similarly, the host galaxies of the calibration set were also separated into host galaxies that rotate with and against the rotation direction of the Milky Way, providing nine galaxies of each. The analysis was done by using the code in `https://github.com/nanditakhetan/SBF_SNeIa_H0`. Table 15 amd Figure 4 show the H_o computed when using the full set of galaxies, just galaxies that rotate in the same direction relative to the Milky Way, and just galaxies spinning in the opposite direction relative to the Milky Way.

As the table shows, the H_o computed with the entire set showed a H_o of 73.758±1.943. That value is in tension with the H_o determined by the CMB. But when using just host galaxies that rotate in the same direction as the Milky Way, the H_o is reduced to 69.049±3.42. That does not fully solve the tension with the H_o determined by the CMB of 67.7 $km/sMpc^{-1}$, but it reduces the tension. But even if the Doppler shift is indeed related to the H_o tension, the H_o is still expected to be higher since the host galaxies are not exactly on the Galactic pole, do not rotate in the exact same rotational velocity as the Milky Way, and their inclinations vary. When using just host galaxies that rotate in the opposite direction relative to the Milky Way, the H_o tension increases to 74.182±3.2, providing another evidence of a link between the H_o tension and the rotational velocity of the host galaxies.

When using just Ia supernovae in galaxies that rotate in the same direction relative to the Milky Way, the tension with the H_o determined by the CMB is reduced, and is within the statistical error. On the other hand, the lower number of data points increases the error, and due to the larger error of the original data the difference is still within the 3% error range. Therefore, these simple experiments may not be considered as a proof, and further analysis with more data will be needed. But the results agree with the observation that rotational velocity can affect the apparent brightness of objects. A link between the rotation directions of the host galaxies of Ia supernovae relative to the Milky Way can also provide a possible explanation to the anisotropy observed in the acceleration of the Universe, observed through Ia supernovae (Javanmardi et al., 2015).

9 Conclusions

The results show that in the fields around the galactic pole galaxies that spin clockwise have a different brightness than galaxies that spin counterclockwise. The inverse difference in the opposite ends of the galactic pole shows that the observations in the both ends are in agreement with the spin direction of the Milky Way. Clearly, a galaxy that seem to spin clockwise in the Northern galactic pole spins in the same direction as galaxies that seem to spin counterclockwise in the Southern galactic pole, and vice versa. The control fields that are

90^o from the galactic pole show no significant difference between galaxies spinning in opposite directions, which provides a certain indication of a correlation between the galactic pole and the magnitude difference. The contention that relativistic beaming can lead to a certain statistical asymmetry when observing a population of galaxies is not unexpected (Alam et al., 2017).

Future and more powerful telescopes such as the Vera C. Rubin Observatory will allow better profiling of such difference. In case the maximum magnitude difference is greater than the maximum expected difference under optimal conditions, that observation can be related to modified Newtonian dynamics, or to relativistic beaming of gravity as an explanation to the galaxy rotation curve anomaly (Blake, 2021). It can also be related to the observation of disagreement between the observed and expected velocity of halo spin (Libeskind et al., 2013).

The observed difference between the magnitude of galaxies that spin in opposite directions had also been observed in previous studies (Shamir, 2016, 2017a,b, 2020a), showing differences between galaxies that spin in opposite directions in the same field. These studies were based on far smaller datasets collected by sky surveys that did not cover the fields around both galactic poles. The data collected by DECam and available through the DESI Legacy Survey allows direct comparison of the differences in brightness between the two ends of the galactic pole. These differences can be related to the effect of relativistic beaming, but further research will be required with more powerful instruments to quantify and profile the magnitude difference.

9.1 Large-scale structure explanation

Another possible explanation to the observation can be an anomaly in the large-scale structure of the Universe. According to that explanation, the axis observed around the galactic pole as shown here is not necessarily the result of differences between the brightness of galaxies as observed from Earth, but a large-scale alignment in the spin directions of galaxies in the Universe. That explanation requires modification to the standard cosmological model, which relies on the assumption that the Universe is isotropic and homogeneous, That assumption is part of the *Cosmological Principle*.

While the Cosmological Principle is a common working assumption for most cosmological models, it has not been fully proven. In fact, multiple probes have shown evidence of violation of the cosmological principle (Aluri et al., 2023). Perhaps the most notable probe is the cosmic microwave background radiation, also exhibiting a cosmological-scale axis (Abramo et al., 2006; Mariano and Perivolaropoulos, 2013; Land and Magueijo, 2005; Ade et al., 2014; Santos et al., 2015; Gruppuso et al., 2018; Yeung and Chu, 2022). It has been suggested that the axis exhibited by the cosmic microwave background radiation agrees with other axes formed by probes such as dark energy and dark flow (Mariano and Perivolaropoulos, 2013). Other anomalies related to the cosmic microwave background radiation are the quandrupole-octopole alignment (Schwarz et al., 2004; Ralston and Jain, 2004; Copi et al., 2007, 2010, 2015), the asymmetry between hemispheres (Eriksen et al., 2004; Land and Magueijo, 2005; Akrami et al., 2014), and the point-parity asymmetry (Kim and Naselsky, 2010b,a). Another related observation is the CMB cold spot (Cruz et al., 2007; Masina and Notari, 2009; Vielva, 2010; Mackenzie et al., 2017; Farhang and Movahed, 2021). It has also been suggested that the isotropy observed with the CMB radiation is not statistically significant (Bennett et al., 2011).

In addition to the CMB, probes that show anisotropy include radio sources (Ghosh et al., 2016; Tiwari and Jain, 2015; Tiwari and Nusser, 2016; Singal, 2019; Marcha and Browne, 2021), LX-T scaling (Migkas et al., 2020), short gamma ray bursts (Mészáros, 2019), acceleration rates (Perivolaropoulos, 2014; Migkas et al., 2021; Krishnan et al., 2022), Ia supernova (Javanmardi et al., 2015; Lin et al., 2016), distribution of galaxy morphology types (Javanmardi and Kroupa, 2017), dark energy (Adhav et al., 2011; Adhav, 2011; Perivolaropoulos, 2014; Colin et al., 2019), fine structure constant (Webb et al., 2011), galaxy motion (Skeivalas et al., 2021), H_o (Luongo et al., 2022), polarization of quasars (Hutsemekers, 1998; Hutsemékers et al., 2005; Secrest et al., 2021; Zhao and Xia, 2021; Semenaite et al., 2021), and cosmic rays (Sommers, 2001; Deligny and Salamida, 2013; Aab et al., 2017, 2019). It has also been shown that the large-scale distribution of galaxies in the Universe is not random (Jones et al., 2005), and could have a preferred direction (Longo, 2011; Shamir, 2012, 2019, 2020c,b, 2021b, 2022c,b; Philcox, 2022; Hou et al., 2022). These probes might not agree with the standard models (Pecker, 1997; Perivolaropoulos, 2014; Bull et al., 2016; Velten and Gomes, 2020; Krishnan et al., 2022, 2021; Luongo et al., 2022; Colgáin, 2022; Abdalla et al., 2022)

The contention of a cosmological-scale axis agrees with cosmological theories that shift from the standard models. For instance, black hole cosmology (Pathria, 1972; Stuckey, 1994; Easson and Brandenberger, 2001; Seshavatharam, 2010; Popławski, 2010; Christillin, 2014; Dymnikova, 2019; Chakrabarty et al., 2020; Popławski, 2021; Seshavatharam and Lakshminarayana, 2022; Gaztanaga, 2022a,b) is a cosmological theory aligned with the contention of the existence of a large-scale axis. Black holes are born from the collapse of a star, and since stars spin black holes also spin (Gammie et al., 2004; Takahashi, 2004; Volonteri et al., 2005; McClintock et al., 2006; Mudambi et al., 2020; Reynolds, 2021). Supermassive black holes are also expected to spin (Montero et al., 2012), and observations of supermassive black holes showed that supermassive black holes spin (Reynolds, 2019). An early example of such observation is the spin of the supermassive black hole of NGC 1365 (Reynolds, 2013). Since black holes spin, if the Universe is the interior of a back hole it is expected to spin around a major axis inherited from the black hole. That observation is aligned with the agreement between the Hubble radius of the Universe and the Schwarzschild radius of a black hole such that the mass of the black hole is the mass of the Universe (Christillin, 2014). Black hole cosmology is a theory under the category of multiverse (Carr and Ellis, 2008; Hall and Nomura, 2008; Antonov, 2015; Garriga et al., 2016), which is one of the first cosmological paradigms (Trimble, 2009; Kragh, 2009).

In addition to black hole cosmology, other models that rely on the presence of a Hubble-scale axis have been proposed. Some of these theories are based on alternative geometrical models such as ellipsoidal universe (Campanelli et al., 2006,

2007, 2011; Gruppuso, 2007; Cea, 2014), flat space cosmology (Tatum et al., 2015a,b, 2018; Azarnia et al., 2021), geometric inflation (Arciniega et al., 2020a; Edelstein et al., 2020; Arciniega et al., 2020b; Jaime, 2021), supersymmetric flows (Rajpoot and Vacaru, 2017), and rotating universe (Gödel, 1949; Ozsváth and Schücking, 1962; Ozsvath and Schücking, 2001; Su and Chu, 2009; Sivaram and Arun, 2012; Chechin, 2016, 2017; Seshavatharam and Lakshminarayana, 2020; Campanelli, 2021). Other theories are double inflation (Feng and Zhang, 2003), f($\mathscr{R}$, $\mathscr{L}_m$) gravity (Kavya et al., 2022), contraction prior to inflation (Piao et al., 2004), primordial anisotropic vacuum pressure (Rodrigues, 2008), moving dark energy (Beltran Jimenez and Maroto, 2007), multiple vacua (Piao, 2005), and spinor-driven inflation (Bohmer and Mota, 2008). While these theories can be considered alternative to the standard cosmological model, they provide explanations to the presence of a Hubble-scale axis. Since the standard model has not been fully proven, alternative theories to the standard cosmology should also be considered.

10 Discussion

Despite decades of intensive research efforts, the physical nature of galaxy rotation is still an unsolved question. The common possible explanations are that the distribution and quantity of the mass of galaxies does not fit its physical properties (dark matter), or that the laws of physics are different when applied to galaxies. This paper proposes the contention that the rotational velocity of the galaxy does not fit its physical properties, and corresponds to a much higher rotational velocity. The explanation is driven by the observation that galaxies that spin in the same direction as the Milky Way have different brightness compared to galaxies that spin in the opposite direction. While the observation does not explain directly the galaxy rotation curve anomaly, it shows another tension between the expected and observed physical properties of galaxy rotation.

While such difference in magnitude can be explained by Doppler shift, the difference is expected to be small. The observed difference is far greater than the expected difference, and it is observable with Earth-based telescopes. A possible explanation is that the physics of galaxy rotation corresponds to a far higher rotational velocity than the observed velocity. While that explanation is physically provocative, the physics of galaxy rotation is still unexplained, and does not follow known or proven physical theories. For instance, the absence of Keplerian velocity decrease in the galaxy rotation curve was ignored for several decades, also because it did not agree with the physical theories (Rubin, 2000).

The tension between galaxy rotational velocity and its physical properties is one of many other possible explanations to the observation of different brightness for galaxies spinning in opposite directions. Another possible explanation discussed here is a possible anomaly in the large-scale structure. In that case, the difference in brightness is not driven by the perspective of an Earth-based observer, but reflects the real structure of the Universe. Other explanations not considered in this paper can also be possible, and might be related to astronomical reasons, as well as certain unknown instrumentation or atmospheric effects.

The link between the rotational velocity of a galaxy and the apparent brightness of its objects can also be related to measurements made with Ia supernovae. Measurements with Ia supernovae have provided unexpected results, and have been shown to be in disagreement with other measurements. For instance, the H_o tension suggests that the CMB or Ia supernovae do not match, and since both are applied to the same Universe it can be assumed that one of these measurements is inaccurate. If the brightness of an Ia supernovae depends on the rotational velocity of the galaxy that hosts it, and the galaxy may not necessarily spin in the same direction as the Milky Way, that can lead to slight changes in the apparent magnitude of the supernovae. Because the distance of an Ia supernovae is determined from its brightness, unexpected changes in the apparent magnitude can lead to a slightly different distance, and consequently to a slightly different H_o. The initial observation of the accelerated expansion of the Universe was also made with Ia supernovae, and such changes in brightness can also have a certain impact on these results.

References

Aab, A., Abreu, P., Aglietta, M., Al Samarai, I., Albuquerque, I., Allekotte, I., Almela, A., Castillo, J. A., Alvarez-Muñiz, J., Anastasi, G. A., et al. (2017). Observation of a large-scale anisotropy in the arrival directions of cosmic rays above 8× 1018 ev. *Science*, 357(6357):1266–1270.

Aab, A., Abreu, P., Aglietta, M., Albuquerque, I., Albury, J. M., Allekotte, I., Almela, A., Castillo, J. A., Alvarez-Muñiz, J., Anastasi, G. A., et al. (2019). Probing the origin of ultra-high-energy cosmic rays with neutrinos in the eev energy range using the pierre auger observatory. *Journal of Cosmology and Astroparticle Physics*, 2019(10):022.

Abbott, T., Abdalla, F., Allam, S., Amara, A., Annis, J., Armstrong, R., Bacon, D., Banerji, M., Bauer, A., Baxter, E., et al. (2016). Cosmology from cosmic shear with dark energy survey science verification data. *Physical Review D*, 94(2):022001.

Abdalla, E., Abellán, G. F., Aboubrahim, A., Agnello, A., Akarsu, Ö., Akrami, Y., Alestas, G., Aloni, D., Amendola, L., Anchordoqui, L. A., et al. (2022). Cosmology intertwined: A review of the particle physics, astrophysics, and cosmology associated with the cosmological tensions and anomalies. *Journal of High Energy Astrophysics*.

Abramo, L. R., Sodré Jr, L., and Wuensche, C. A. (2006). Anomalies in the low cmb multipoles and extended foregrounds. *Physical Review D*, 74(8):083515.

Ade, P. A., Aghanim, N., Armitage-Caplan, C., Arnaud, M., Ashdown, M., Atrio-Barandela, F., Aumont, J., Baccigalupi, C., Banday, A. J., Barreiro, R., et al. (2014). Planck 2013 results. xxiii. isotropy and statistics of the cmb. *Astronomy & Astrophysics*, 571:A23.

Adhav, K. (2011). Lrs bianchi type-i universe with anisotropic dark energy in lyra geometry. *International Journal of Astronomy and Astrophysics*, 1(4):204–209.

Adhav, K., Bansod, A., Wankhade, R., and Ajmire, H. (2011). Kantowski-sachs cosmological models with anisotropic dark energy. *Open Physics*, 9(4):919–925.

Akerib, D. S., Alsum, S., Araújo, H. M., Bai, X., Bailey, A. J., Balajthy, J., Beltrame, P., Bernard, E. P., Bernstein, A., Biesiadzinski, T. P., Boulton, E. M., Bramante, R., Brás, P., Byram, D., Cahn, S. B., Carmona-Benitez, M. C., Chan, C., Chiller, A. A., Chiller, C., Currie, A., Cutter, J. E., Davison, T. J. R., Dobi, A., Dobson, J. E. Y., Druszkiewicz, E., Edwards, B. N., Faham, C. H., Fiorucci, S., Gaitskell, R. J., Gehman, V. M., Ghag, C., Gibson, K. R., Gilchriese, M. G. D., Hall, C. R., Hanhardt, M., Haselschwardt, S. J., Hertel, S. A., Hogan, D. P., Horn, M., Huang, D. Q., Ignarra, C. M., Ihm, M., Jacobsen, R. G., Ji, W., Kamdin, K., Kazkaz, K., Khaitan, D., Knoche, R., Larsen, N. A., Lee, C., Lenardo, B. G., Lesko, K. T., Lindote, A., Lopes, M. I., Manalaysay, A., Mannino, R. L., Marzioni, M. F., McKinsey, D. N., Mei, D.-M., Mock, J., Moongweluwan, M., Morad, J. A., Murphy, A. S. J., Nehrkorn, C., Nelson, H. N., Neves, F., O'Sullivan, K., Oliver-Mallory, K. C., Palladino, K. J., Pease, E. K., Phelps, P., Reichhart, L., Rhyne, C., Shaw, S., Shutt, T. A., Silva, C., Solmaz, M., Solovov, V. N., Sorensen, P., Stephenson, S., Sumner, T. J., Szydagis, M., Taylor, D. J., Taylor, W. C., Tennyson, B. P., Terman, P. A., Tiedt, D. R., To, W. H., Tripathi, M., Tvrznikova, L., Uvarov, S., Verbus, J. R., Webb, R. C., White, J. T., Whitis, T. J., Witherell, M. S., Wolfs, F. L. H., Xu, J., Yazdani, K., Young, S. K., and Zhang, C. (2017). Results from a search for dark matter in the complete lux exposure. *Phys. Rev. Lett.*, 118:021303.

Akrami, Y., Fantaye, Y., Shafieloo, A., Eriksen, H., Hansen, F. K., Banday, A. J., and Górski, K. M. (2014). Power asymmetry in wmap and planck temperature sky maps as measured by a local variance estimator. *Astrophysical Journal Letters*, 784(2):L42.

Alam, S., Croft, R. A., Ho, S., Zhu, H., and Giusarma, E. (2017). Relativistic effects on galaxy redshift samples due to target selection. *Monthyl Notices of the Royal Astronomical Society*, 471(2):2077–2087.

Aluri, P. K., Cea, P., Chingangbam, P., Chu, M.-C., Clowes, R. G., Hutsemékers, D., Kochappan, J. P., Krasiński, A., Lopez, A. M., Liu, L., Martens, N. C. M., Martins, C. J. A. P., Migkas, K., Colgáin, E. ., Pranav, P., Shamir, L., Singal, A. K., Sheikh-Jabbari, M. M., Wagner, J., Wang, S.-J., Wiltshire, D. L., Yeung, S., Yin, L., and Zhao, W. (2023). Is the observable universe consistent with the cosmological principle? *Classical and Quantum Gravity*, 40(9):094001.

Antonov, A. A. (2015). Hidden multiverse. *International Journal of Advanced Research in Physical Science*, 2(1):25–32.

Aprile, E., Aalbers, J., Agostini, F., Alfonsi, M., Althueser, L., Amaro, F. D., Anthony, M., Arneodo, F., Baudis, L., Bauermeister, B., Benabderrahmane, M. L., Berger, T., Breur, P. A., Brown, A., Brown, A., Brown, E., Bruenner, S., Bruno, G., Budnik, R., Capelli, C., Cardoso, J. M. R., Cichon, D., Coderre, D., Colijn, A. P., Conrad, J., Cussonneau, J. P., Decowski, M. P., de Perio, P., Di Gangi, P., Di Giovanni, A., Diglio, S., Elykov, A., Eurin, G., Fei, J., Ferella, A. D., Fieguth, A., Fulgione, W., Gallo Rosso, A., Galloway, M., Gao, F., Garbini, M., Geis, C., Grandi, L., Greene, Z., Qiu, H., Hasterok, C., Hogenbirk, E., Howlett, J., Itay, R., Joerg, F., Kaminsky, B., Kazama, S., Kish, A., Koltman, G., Landsman, H., Lang, R. F., Levinson, L., Lin, Q., Lindemann, S., Lindner, M., Lombardi, F., Lopes, J. A. M., Mahlstedt, J., Manfredini, A., Marrodán Undagoitia, T., Masbou, J., Masson, D., Messina, M., Micheneau, K., Miller, K., Molinario, A., Morå, K., Murra, M., Naganoma, J., Ni, K., Oberlack, U., Pelssers, B., Piastra, F., Pienaar, J., Pizzella, V., Plante, G., Podviianiuk, R., Priel, N., Ramírez García, D., Rauch, L., Reichard, S., Reuter, C., Riedel, B., Rizzo, A., Rocchetti, A., Rupp, N., dos Santos, J. M. F., Sartorelli, G., Scheibelhut, M., Schindler, S., Schreiner, J., Schulte, D., Schumann, M., Scotto Lavina, L., Selvi, M., Shagin, P., Shockley, E., Silva, M., Simgen, H., Thers, D., Toschi, F., Trinchero, G., Tunnell, C., Upole, N., Vargas, M., Wack, O., Wang, H., Wang, Z., Wei, Y., Weinheimer, C., Wittweg, C., Wulf, J., Ye, J., Zhang, Y., and Zhu, T. (2018). Dark matter search results from a one ton-year exposure of xenon1t. *Phys. Rev. Lett.*, 121:111302.

Arciniega, G., Bueno, P., Cano, P. A., Edelstein, J. D., Hennigar, R. A., and Jaime, L. G. (2020a). Geometric inflation. *Physics Letters B*, 802:135242.

Arciniega, G., Edelstein, J. D., and Jaime, L. G. (2020b). Towards geometric inflation: the cubic case. *Physics Letters B*, 802:135272.

Arun, K., Gudennavar, S., and Sivaram, C. (2017). Dark matter, dark energy, and alternate models: A review. *Advances in Space Research*, 60(1):166–186.

Azarnia, S., Fareghbal, R., Naseh, A., and Zolfi, H. (2021). Islands in flat-space cosmology. *Physical Review D*, 104(12):126017.

Babcock, H. W. (1939). The rotation of the andromeda nebula. *Lick Observatory Bulletin*, 19:41–51.

Beltran Jimenez, J. and Maroto, A. L. (2007). Cosmology with moving dark energy and the cmb quadrupole. *Physical Review D*, 76(2):023003.

Bennett, C., Hill, R., Hinshaw, G., Larson, D., Smith, K., Dunkley, J., Gold, B., Halpern, M., Jarosik, N., Kogut, A., et al. (2011). Seven-year wilkinson microwave anisotropy probe (wmap*) observations: Are there cosmic microwave background anomalies? *ApJS*, 192(2):17.

Berriman, G., Good, J., Laity, A., Bergou, A., Jacob, J., Katz, D., Deelman, E., Kesselman, C., Singh, G., Su, M.-H., et al. (2004). Montage: a grid enabled image mosaic service for the national virtual observatory. In *Astronomical Data Analysis Software and Systems (ADASS) XIII*, volume 314, page 593.

Bertone, G. and Hooper, D. (2018). History of dark matter. *Rev. Mod. Phys.*, 90:045002.

Bertone, G. and Tait, T. M. (2018). A new era in the search for dark matter. *Nature*, 562(7725):51–56.

Blake, B. C. (2021). Relativistic beaming of gravity and the missing mass problem. *Bulletin of the American Physical Society*, page B17.00002.

Bohmer, C. G. and Mota, D. F. (2008). Cmb anisotropies and inflation from non-standard spinors. *Physics Letters B*, 663(3):168–171.

Bolejko, K. (2018). Emerging spatial curvature can resolve the tension between high-redshift cmb and low-redshift distance ladder measurements of the hubble constant. *Physical Review D*, 97(10):103529.

Brout, D. and Daniel, S. (2020). It's dust: Solving the mysteries of the intrinsic scatter and host-galaxy dependence of standardized type ia supernova brightnesses. *arxiv*, page 2004.10206.

Bull, P., Akrami, Y., Adamek, J., Baker, T., Bellini, E., Jimenez, J. B., Bentivegna, E., Camera, S., Clesse, S., Davis, J. H., et al. (2016). Beyond λcdm: Problems, solutions, and the road ahead. *Physics of the Dark Universe*, 12:56–99.

Buta, R. J., Byrd, G. G., and Freeman, T. (2003). The ringed spiral galaxy ngc 4622. i. photometry, kinematics, and the case for two strong leading outer spiral arms. *Astronomical Journal*, 125(2):634.

Byrd, G. and Howard, S. (2019). Ngc 4622: Unusual spiral density waves and calculated disk surface density. *Journal of the Washington Academy of Sciences*, 105(3):1–12.

Byrd, G. and Howard, S. (2021). Spiral galaxies when disks dominate their halos (using arm pitches and rotation curves). *Journal of the Washington Academy of Sciences*, 107(1):1.

Byrd, G. G., Freeman, T., Howard, S., and Buta, R. J. (2007). The ringed spiral galaxy ngc4622. ii. an independent determination that the two outer arms lead. *Astronomical Journal*, 135(1):408.

Camarena, D. and Marra, V. (2018). Impact of the cosmic variance on h 0 on cosmological analyses. *Physical Review D*, 98(2):023537.

Camarena, D. and Marra, V. (2020). Local determination of the hubble constant and the deceleration parameter. *Physical Review Research*, 2(1):013028.

Campanelli, L. (2021). A conjecture on the neutrality of matter. *Foundations of Physics*, 51:56.

Campanelli, L., Cea, P., Fogli, G., and Tedesco, L. (2011). Cosmic parallax in ellipsoidal universe. *Modern Physics Letters A*, 26(16):1169–1181.

Campanelli, L., Cea, P., and Tedesco, L. (2006). Ellipsoidal universe can solve the cosmic microwave background quadrupole problem. *PRL*, 97(13):131302.

Campanelli, L., Cea, P., and Tedesco, L. (2007). Cosmic microwave background quadrupole and ellipsoidal universe. *Physical Review D*, 76(6):063007.

Capak, P., Aussel, H., Ajiki, M., McCracken, H., Mobasher, B., Scoville, N., Shopbell, P., Taniguchi, Y., Thompson, D., Tribiano, S., et al. (2007). The first release cosmos optical and near-ir data and catalog. *Astrophysical Journal Supplement Series*, 172(1):99.

Capozziello, S. and De Laurentis, M. (2012). The dark matter problem from f (r) gravity viewpoint. *Annalen der Physik*, 524(9-10):545–578.

Carr, B. and Ellis, G. (2008). Universe or multiverse? *Astronomy & Geophysics*, 49(2):2–29.

Carroll, S. M., Sawicki, I., Silvestri, A., and Trodden, M. (2006). Modified-source gravity and cosmological structure formation. *New Journal of Physics*, 8(12):323.

Cea, P. (2014). The ellipsoidal universe in the planck satellite era. *Monthly Notices of the Royal Astronomical Society*, 441(2):1646–1661.

Chadwick, E. A., Hodgkinson, T. F., and McDonald, G. S. (2013). Gravitational theoretical development supporting mond. *Physical Review D*, 88(2):024036.

Chakrabarty, H., Abdujabbarov, A., Malafarina, D., and Bambi, C. (2020). A toy model for a baby universe inside a black hole. *European Physical Journal C*, 80(1909.07129):1–10.

Chechin, L. (2016). Rotation of the universe at different cosmological epochs. *Astronomy Reports*, 60(6):535–541.

Chechin, L. (2017). Does the cosmological principle exist in the rotating universe? *Gravitation and Cosmology*, 23(4):305–310.

Christillin, P. (2014). The machian origin of linear inertial forces from our gravitationally radiating black hole universe. *The European Physical Journal Plus*, 129(8):1–3.

Colgáin, E. Ó. (2022). Probing the anisotropic universe with gravitational waves. *arXiv:2203.03956*.

Colin, J., Mohayaee, R., Rameez, M., and Sarkar, S. (2019). Evidence for anisotropy of cosmic acceleration. *Astronomy & Astrophysics*, 631:L13.

Copi, C. J., Huterer, D., Schwarz, D. J., and Starkman, G. D. (2007). Uncorrelated universe: statistical anisotropy and the vanishing angular correlation function in wmap years 1–3. *Physical Review D*, 75(2):023507.

Copi, C. J., Huterer, D., Schwarz, D. J., and Starkman, G. D. (2010). Large-angle anomalies in the cmb. *Advances in Astronomy*, 2010.

Copi, C. J., Huterer, D., Schwarz, D. J., and Starkman, G. D. (2015). Large-scale alignments from wmap and planck. *Monthly Notices of the Royal Astronomical Society*, 449(4):3458–3470.

Cruz, M., Cayon, L., Martinez-Gonzalez, E., Vielva, P., and Jin, J. (2007). The non-gaussian cold spot in the 3-year wmap data. *Astrophysical Journal*, 655(11).

Davis, D. R. and Hayes, W. B. (2014). SpArcFiRe: Scalable Automated Detection of Spiral Galaxy Arm Segments. *Astrophysical Journal*, 790(2):87.

Davis, T. M., Hinton, S. R., Howlett, C., and Calcino, J. (2019). Can redshift errors bias measurements of the hubble constant? *Monthly Notices of the Royal Astronomical Society*, 490(2):2948–2957.

De Blok, W. and McGaugh, S. (1998). Testing modified newtonian dynamics with low surface brightness galaxies: rotation curve fits. *Astrophysical Journal*, 508(1):132.

De Vaucouleurs, G. (1959). General physical properties of external galaxies. In *Astrophysik IV: Sternsysteme/Astrophysics IV: Stellar Systems*, pages 311–372. Springer.

Deligny, O. and Salamida, F. (2013). Searches for large-scale anisotropies of cosmic rays: Harmonic analysis and shuffling technique. *Astroparticle Physics*, 46:40–49.

Dey, A., Schlegel, D. J., Lang, D., Blum, R., Burleigh, K., Fan, X., Findlay, J. R., Finkbeiner, D., Herrera, D., Juneau, S., et al. (2019). Overview of the desi legacy imaging surveys. *Astronomical Journal*, 157(5):168.

Dhar, S. and Shamir, L. (2022). Systematic biases when using deep neural networks for annotating large catalogs of astronomical images. *Astronomy and Computing*, 38:100545.

Di Valentino, E., Anchordoqui, L. A., Akarsu, Ö., Ali-Haimoud, Y., Amendola, L., Arendse, N., Asgari, M., Ballardini, M., Basilakos, S., Battistelli, E., et al. (2021a). Snowmass2021-letter of interest cosmology intertwined ii: The hubble constant tension. *Astroparticle Physics*, 131:102605.

Di Valentino, E., Anchordoqui, L. A., Akarsu, Ö., Ali-Haimoud, Y., Amendola, L., Arendse, N., Asgari, M., Ballardini, M., Basilakos, S., Battistelli, E., et al. (2021b). Snowmass2021-letter of interest cosmology intertwined iv: The age of the universe and its curvature. *Astroparticle Physics*, 131:102607.

Di Valentino, E., Mena, O., Pan, S., Visinelli, L., Yang, W., Melchiorri, A., Mota, D. F., Riess, A. G., and Silk, J. (2021c). In the realm of the hubble tension—a review of solutions. *Classical and Quantum Gravity*, 38(15):153001.

Díaz-Saldaña, I., López-Domínguez, J., and Sabido, M. (2018). On emergent gravity, black hole entropy and galactic rotation curves. *Physics of the Dark Universe*, 22:147–151.

Dixon, M., Lidman, C., Mould, J., Kelsey, L., Brout, D., Möller, A., Wiseman, P., Sullivan, M., Galbany, L., Davis, T. M., Vincenzi, M., Scolnic, D., Lewis, G. F., Smith, M., Kessler, R., Duffy, A., Taylor, E. N., Flynn, C., Abbott, T. M. C., Aguena, M., Allam, S., Andrade-Oliveira, F., Annis, J., Asorey, J., Bertin, E., Bocquet, S., Brooks, D., Burke, D. L., Carnero Rosell, A., Carollo, D., Carrasco Kind, M., Carretero, J., Costanzi, M., da Costa, L. N., Pereira, M. E. S., Doel, P., Everett, S., Ferrero, I., Flaugher, B., Friedel, D., Frieman, J., García-Bellido, J., Gatti, M., Gerdes, D. W., Glazebrook, K., Gruen, D., Gschwend, J., Gutierrez, G., Hinton, S. R., Hollowood, D. L., Honscheid, K., Huterer, D., James, D. J., Kuehn, K., Kuropatkin, N., Malik, U., March, M., Menanteau, F., Miquel, R., Morgan, R., Nichol, B., Ogando, R. L. C., Palmese, A., Paz-Chinchón, F., Pieres, A., Plazas Malagón, A. A., Rodriguez-Monroy, M., Romer, A. K., Sanchez, E., Scarpine, V., Sevilla-Noarbe, I., Soares-Santos, M., Suchyta, E., Tarle, G., To, C., Tucker, B. E., Tucker, D. L., and Varga, T. N. (2022). Using host galaxy spectroscopy to explore systematics in the standardization of type ia supernovae. *Monthly Notices of the Royal Astronomical Society*, 517(3):4291–4304.

Dodelson, S. (2011). The real problem with mond. *International Journal of Modern Physics D*, 20(14):2749–2753.

Dojcsak, L. and Shamir, L. (2014). Quantitative analysis of spirality in elliptical galaxies. *New Astronomy*, 28:1–8.

Donato, F., Gentile, G., Salucci, P., Frigerio Martins, C., Wilkinson, M., Gilmore, G., Grebel, E., Koch, A., and Wyse, R. (2009). A constant dark matter halo surface density in galaxies. *Monthly Notices of the Royal Astronomical Society*, 397(3):1169–1176.

Driver, S. P. and Robotham, A. S. (2010). Quantifying cosmic variance. *Monthyl Notices of the Royal Astronomical Society*, 407(4):2131–2140.

Dymnikova, I. (2019). Universes inside a black hole with the de sitter interior. *Universe*, 5(5):111.

Easson, D. A. and Brandenberger, R. H. (2001). Universe generation from black hole interiors. *Journal of High Energy Physics*, 2001(06):024.

Edelstein, J. D., Rodríguez, D. V., and López, A. V. (2020). Aspects of geometric inflation. *JCAP*, 2020(12):040.

Eriksen, H. K., Hansen, F. K., Banday, A. J., Gorski, K. M., and Lilje, P. B. (2004). Asymmetries in the cosmic microwave background anisotropy field. *Astrophysical Journal*, 605(1):14.

Falcon, N. (2021). A large-scale heuristic modification of newtonian gravity as an alternative approach to dark energy and dark matter. *Journal of Astrophysics and Astronomy*, 42(2):1–13.

Farhang, M. and Movahed, S. (2021). Cmb cold spot in the planck light. *Astrophysical Journal*, 906(1):41.

Farnes, J. S. (2018). A unifying theory of dark energy and dark matter: Negative masses and matter creation within

a modified λcdm framework. *Astronomy & Astrophysics*, 620:A92.

Feng, B. and Zhang, X. (2003). Double inflation and the low cmb quadrupole. *Physics Letters B*, 570(3-4):145–150.

Flaugher, B. L., Abbott, T. M., Angstadt, R., Annis, J., Antonik, M. L., Bailey, J., Ballester, O., Bernstein, J. P., Bernstein, R. A., Bonati, M., et al. (2012). Status of the dark energy survey camera (decam) project. In *Ground-based and Airborne Instrumentation for Astronomy IV*, volume 8446, pages 343–357. SPIE.

Freeman, T., Byrd, G., and Howard, S. (1991). Simulating ngc 4622: A leading-arm spiral galaxy. In *BASS*, volume 23, page 1460.

Gammie, C. F., Shapiro, S. L., and McKinney, J. C. (2004). Black hole spin evolution. *Astrophysical Journal*, 602(1):312.

Garriga, J., Vilenkin, A., and Zhang, J. (2016). Black holes and the multiverse. *JCAP*, 2016(02):064.

Gaztanaga, E. (2022a). The black hole universe, part i. *Symmetry*, 14(9):1849.

Gaztanaga, E. (2022b). The black hole universe, part ii. *Symmetry*, 14(10):1984.

Ghosh, S., Jain, P., Kashyap, G., Kothari, R., Nadkarni-Ghosh, S., and Tiwari, P. (2016). Probing statistical isotropy of cosmological radio sources using square kilometre array. *JOAA*, 37(4):1–21.

Gödel, K. (1949). An example of a new type of cosmological solutions of einstein's field equations of gravitation. *Reviews of Modern Physics*, 21(3):447.

Gomel, R. and Zimmerman, T. (2021). The effects of inertial forces on the dynamics of disk galaxies. *Galaxies*, 9(2):34.

Gruppuso, A. (2007). Complete statistical analysis for the quadrupole amplitude in an ellipsoidal universe. *Physical Review D*, 76(8):083010.

Gruppuso, A., Kitazawa, N., Lattanzi, M., Mandolesi, N., Natoli, P., and Sagnotti, A. (2018). The evens and odds of cmb anomalies. *Physics of the Dark Universe*, 20:49–64.

Hall, L. J. and Nomura, Y. (2008). Evidence for the multiverse in the standard model and beyond. *Physical Review D*, 78(3):035001.

Haug, E. G. (2022). Does lorentz relativistic mass make dark energy superfluous? *Universe*, 8(11):577.

Hayes, W. B., Davis, D., and Silva, P. (2017). On the nature and correction of the spurious s-wise spiral galaxy winding bias in galaxy zoo 1. *Monthyl Notices of the Royal Astronomical Society*, 466(4):3928–3936.

Helmert, F. (1876). Die genauigkeit der formel von peters zur berechnung des wahrscheinlichen beobachtungsfehlers director beobachtungen gleicher genauigkeit. *Astronomical Notes*, 88:113.

Hirata, C. M., Mandelbaum, R., Ishak, M., Seljak, U., Nichol, R., Pimbblet, K. A., Ross, N. P., and Wake, D. (2007). Intrinsic galaxy alignments from the 2slaq and sdss surveys: luminosity and redshift scalings and implications for weak lensing surveys. *Monthly Notices of the Royal Astronomical Society*, 381(3):1197–1218.

Hofmeister, A. M. and Criss, R. E. (2020). Debate on the physics of galactic rotation and the existence of dark matter.

Hou, J., Slepian, Z., and Cahn, R. N. (2022). Measurement of parity-odd modes in the large-scale 4-point correlation function of sdss boss dr12 cmass and lowz galaxies. *arXiv:2206.03625*.

Hutsemekers, D. (1998). Evidence for very large-scale coherent orientations of quasar polarization vectors. *Astronomy & Astrophysics*, 332:410–428.

Hutsemékers, D., Cabanac, R., Lamy, H., and Sluse, D. (2005). Mapping extreme-scale alignments of quasar polarization vectors. *Astronomy & Astrophysics*, 441(3):915–930.

Iocco, F., Pato, M., and Bertone, G. (2015). Testing modified newtonian dynamics in the milky way. *Physical Review D*, 92(8):084046.

Jaime, L. G. (2021). On the viability of the evolution of the universe with geometric inflation. *Physics of the Dark Universe*, 34:100887.

Javanmardi, B. and Kroupa, P. (2017). Anisotropy in the all-sky distribution of galaxy morphological types. *Astronomy & Astrophysics*, 597:A120.

Javanmardi, B., Porciani, C., Kroupa, P., and Pflam-Altenburg, J. (2015). Probing the isotropy of cosmic acceleration traced by type ia supernovae. *Astrophysical Journal*, 810(1):47.

Jones, B. J., Martínez, V. J., Saar, E., and Trimble, V. (2005). Scaling laws in the distribution of galaxies. *Reviews of Modern Physics*, 76(4):1211.

Kamionkowski, M. and Loeb, A. (1997). Getting around cosmic variance. *Physical Review D*, 56(8):4511.

Kavya, N., Venkatesha, V., Mandal, S., and Sahoo, P. (2022). Constraining anisotropic cosmological model in f($\mathscr{R}$, $\mathscr{L}_m$) gravity. *Physics of the Dark Universe*, 38:101126.

Keenan, R. P., Marrone, D. P., and Keating, G. K. (2020). Biases and cosmic variance in molecular gas abundance measurements at high redshift. *Astrophysical Journal*, 904(2):127.

Khetan, N., Izzo, L., Branchesi, M., Wojtak, R., Cantiello, M., Murugeshan, C., Agnello, A., Cappellaro, E., Della Valle, M., Gall, C., Hjorth, J., Benetti, S., Brocato, E., Burke, J., Hiramatsu, D., Howell, D. A., Tomasella, L., and Valenti, S. (2021). A new measurement of the hubble constant using type ia supernovae calibrated with surface brightness fluctuations. *Astronomy & Astrophysics*, 647:A72.

Kim, J. and Naselsky, P. (2010a). Anomalous parity asymmetry of the wilkinson microwave anisotropy probe power spectrum data at low multipoles. *Astrophysical Journal Letters*, 714(2):L265.

Kim, J. and Naselsky, P. (2010b). Anomalous parity asymmetry of wmap 7-year power spectrum data at low multipoles: is it cosmological or systematics? *Physical Review D*, 82(6):063002.

Koekemoer, A. M., Aussel, H., Calzetti, D., Capak, P., Giavalisco, M., Kneib, J.-P., Leauthaud, A., Le Fevre, O., McCracken, H., Massey, R., et al. (2007). The cosmos survey: Hubble space telescope advanced camera for surveys observations and data processing. *Astrophysical Journal Supplement Series*, 172(1):196.

Kormendy, J. (1977). Brightness distributions in compact and normal galaxies. ii-structure parameters of the spheroidal component. *Astrophysical Journal*, 218:333–346.

Kragh, H. (2009). Contemporary history of cosmology and the controversy over the multiverse. *Annals of Science*, 66(4):529–551.

Krishnan, C., Mohayaee, R., Colgáin, E. Ó., Sheikh-Jabbari, M., and Yin, L. (2021). Does hubble tension signal a breakdown in flrw cosmology? *Classical and Quantum Gravity*, 38(18):184001.

Krishnan, C., Mohayaee, R., Colgáin, E. Ó., Sheikh-Jabbari, M., and Yin, L. (2022). Hints of flrw breakdown from supernovae. *Physical Review D*, 105(6):063514.

Kroupa, P. (2012). The dark matter crisis: falsification of the current standard model of cosmology. *Publications of the Astronomical Society of Australia*, 29(4):395–433.

Kroupa, P. (2015). Galaxies as simple dynamical systems: observational data disfavor dark matter and stochastic star formation. *Canadian Journal of Physics*, 93(2):169–202.

Kroupa, P., Pawlowski, M., and Milgrom, M. (2012). The failures of the standard model of cosmology require a new paradigm. *International Journal of Modern Physics D*, 21(14):1230003.

Land, K. and Magueijo, J. (2005). Examination of evidence for a preferred axis in the cosmic radiation anisotropy. *PRL*, 95(7):071301.

Larin, S. A. (2022). Towards the explanation of flatness of galaxies rotation curves. *Universe*, 8(12):632.

Libeskind, N. I., Hoffman, Y., Forero-Romero, J., Gottlöber, S., Knebe, A., Steinmetz, M., and Klypin, A. (2013). The velocity shear tensor: tracer of halo alignment. *Monthyl Notices of the Royal Astronomical Society*, 428(3):2489–2499.

Lin, H.-N., Li, X., and Chang, Z. (2016). The significance of anisotropic signals hiding in the type ia supernovae. *Monthyl Notices of the Royal Astronomical Society*, 460(1):617–626.

Lintott, C. J., Schawinski, K., Slosar, A., Land, K., Bamford, S., Thomas, D., Raddick, M. J., Nichol, R. C., Szalay, A., Andreescu, D., et al. (2008). Galaxy zoo: morphologies derived from visual inspection of galaxies from the sloan digital sky survey. *Monthly Notices of the Royal Astronomical Society*, 389(3):1179–1189.

Loeb, A. and Gaudi, B. S. (2003). Periodic flux variability of stars due to the reflex doppler effect induced by planetary companions. *Astrophysical Journal Letters*, 588(2):L117.

Longo, M. J. (2011). Detection of a dipole in the handedness of spiral galaxies with redshifts z 0.04. *Physics Letters B*, 699(4):224–229.

Luongo, O., Muccino, M., Colgáin, E. Ó., Sheikh-Jabbari, M., and Yin, L. (2022). Larger h_0 values in the cmb dipole direction. *Physical Review D*, 105(10):103510.

Mackenzie, R., Shanks, T., Bremer, M. N., Cai, Y.-C., Gunawardhana, M. L., Kovács, A., Norberg, P., and Szapudi, I. (2017). Evidence against a supervoid causing the cmb cold spot. *Monthyl Notices of the Royal Astronomical Society*, 470(2):2328–2338.

Mandelbaum, R., Seljak, U., Kauffmann, G., Hirata, C. M., and Brinkmann, J. (2006). Galaxy halo masses and satellite fractions from galaxy–galaxy lensing in the sloan digital sky survey: stellar mass, luminosity, morphology and environment dependencies. *Monthly Notices of the Royal Astronomical Society*, 368(2):715–731.

Mannheim, P. D. (2006). Alternatives to dark matter and dark energy. *Progress in Particle and Nuclear Physics*, 56(2):340–445.

Marcha, M. J. M. and Browne, I. W. A. (2021). Large-scale clustering amongst Fermi blazars; evidence for axis alignments? *Monthly Notices of the Royal Astronomical Society*, 507(1):1361–1368.

Mariano, A. and Perivolaropoulos, L. (2013). Cmb maximum temperature asymmetry axis: Alignment with other cosmic asymmetries. *Physical Review D*, 87(4):043511.

Masina, I. and Notari, A. (2009). The cold spot as a large void: lensing effect on cmb two and three point correlation functions. *JCAP*, 2009(07):035.

Mayall, N. (1951). *In the structure of the galaxy.* 19. Ann Arbor: Univ. Mich. Press.

McClintock, J. E., Shafee, R., Narayan, R., Remillard, R. A., Davis, S. W., and Li, L.-X. (2006). The spin of the near-extreme kerr black hole grs 1915+ 105. *Astrophysical Journal*, 652(1):518.

Meldorf, C., Palmese, A., Brout, D., Chen, R., Scolnic, D., Kelsey, L., Galbany, L., Hartley, W. G., Davis, T. M., Drlica-Wagner, A., Vincenzi, M., Annis, J., Dixon, M., Graur, O., Lidman, C., Möller, A., Nugent, P., Rose, B., Smith, M., Allam, S., Tucker, D. L., Asorey, J., Calcino, J., Carollo, D., Glazebrook, K., Lewis, G. F., Taylor, G., Tucker, B. E., Kim, A. G., Diehl, H. T., Aguena, M.,

Andrade-Oliveira, F., Bacon, D., Bertin, E., Bocquet, S., Brooks, D., Burke, D. L., Carretero, J., Kind, M. C., Castander, F. J., Costanzi, M., da Costa, L. N., Desai, S., Doel, P., Everett, S., Ferrero, I., Friedel, D., Frieman, J., García-Bellido, J., Gatti, M., Gruen, D., Gschwend, J., Gutierrez, G., Hinton, S. R., Hollowood, D. L., Honscheid, K., James, D. J., Kuehn, K., March, M., Marshall, J. L., Menanteau, F., Miquel, R., Morgan, R., Paz-Chinchón, F., Pereira, M. E. S., Malagón, A. A. P., Sanchez, E., Scarpine, V., Sevilla-Noarbe, I., Suchyta, E., Tarle, G., Varga, T. N., and DES, C. (2022). The dark energy survey supernova program results: Type ia supernova brightness correlates with host galaxy dust. *Monthly Notices of the Royal Astronomical Society*. stac3056.

Mészáros, A. (2019). An oppositeness in the cosmology: Distribution of the gamma ray bursts and the cosmological principle. *Astronomical Notes*, 340(7):564–569.

Migkas, K., Pacaud, F., Schellenberger, G., Erler, J., Nguyen-Dang, N., Reiprich, T., Ramos-Ceja, M., and Lovisari, L. (2021). Cosmological implications of the anisotropy of ten galaxy cluster scaling relations. *Astronomy & Astrophysics*, 649:A151.

Migkas, K., Schellenberger, G., Reiprich, T., Pacaud, F., Ramos-Ceja, M., and Lovisari, L. (2020). Probing cosmic isotropy with a new x-ray galaxy cluster sample through the lx–t scaling relation. *Astronomy & Astrophysics*, 636:A15.

Milgrom, M. (1983). A modification of the newtonian dynamics as a possible alternative to the hidden mass hypothesis. *Astrophysical Journal*, 270:365–370.

Milgrom, M. (2007). Mond and the mass discrepancies in tidal dwarf galaxies. *Astrophysical Journal Letters*, 667(1):L45.

Milgrom, M. (2019). Mond in galaxy groups: A superior sample. *Physical Review D*, 99(4):044041.

Montero, P. J., Janka, H.-T., and Müller, E. (2012). Relativistic collapse and explosion of rotating supermassive stars with thermonuclear effects. *Astrophysical Journal*, 749(1):37.

Morháč, M., Kliman, J., Matoušek, V., Veselskỳ, M., and Turzo, I. (2000). Identification of peaks in multidimensional coincidence γ-ray spectra. *Nuclear Instruments and Methods in Physics Research Section A: Accelerators, Spectrometers, Detectors and Associated Equipment*, 443(1):108–125.

Mörtsell, E. and Dhawan, S. (2018). Does the hubble constant tension call for new physics? *Journal of Cosmology and Astroparticle Physics*, 2018(09):025.

Moster, B. P., Somerville, R. S., Newman, J. A., and Rix, H.-W. (2011). A cosmic variance cookbook. *Astrophysical Journal*, 731(2):113.

Mudambi, S. P., Rao, A., Gudennavar, S., Misra, R., and Bubbly, S. (2020). Estimation of the black hole spin in lmc x-1 using astrosat. *Monthly Notices of the Royal Astronomical Society*, 498(3):4404–4410.

Nagao, S. (2020). Galactic evolution showing a constant circulating speed of stars in a galactic disc without requiring dark matter. *Reports in Advances of Physical Sciences*, 4(02):2050004.

O'Brien, J. G., Chiarelli, T. L., Dentico, J., Stulge, M., Stefanski, B., Moss, R., and Chaykov, S. (2017). Alternative gravity rotation curves for the little things survey. *Astrophysical Journal*, 852(1):6.

Oort, J. H. (1940). Some problems concerning the structure and dynamics of the galactic system and the elliptical nebulae ngc 3115 and 4494. *Astrophysical Journal*, 91:273.

Opik, E. (1922). An estimate of the distance of the andromeda nebula. *Astrophysical Journal*, 55.

Ozsváth, I. and Schücking, E. (1962). Finite rotating universe. *Nature*, 193(4821):1168–1169.

Ozsvath, I. and Schücking, E. (2001). Approaches to gödel's rotating universe. *Classical and Quantum Gravity*, 18(12):2243.

Pandey, S., Raveri, M., and Jain, B. (2020). Model independent comparison of supernova and strong lensing cosmography: Implications for the hubble constant tension. *Physical Review D*, 102(2):023505.

Pathria, R. (1972). The universe as a black hole. *Nature*, 240(5379):298–299.

Pease, F. (1918). The rotation and radial velocity of the central part of the andromeda nebula. *PNAS*, 4(1):21.

Pecker, J.-C. (1997). Some critiques of the big bang cosmology. *JOAA*, 18(4):323–333.

Perivolaropoulos, L. (2014). Large scale cosmological anomalies and inhomogeneous dark energy. *Galaxies*, 2(1):22–61.

Philcox, O. H. (2022). Probing parity-violation with the four-point correlation function of boss galaxies. *arXiv:2206.04227*.

Piao, Y.-S. (2005). Possible explanation to a low cmb quadrupole. *Physical Review D*, 71(8):087301.

Piao, Y.-S., Feng, B., and Zhang, X. (2004). Suppressing the cmb quadrupole with a bounce from the contracting phase to inflation. *Physical Review D*, 69(10):103520.

Pogosian, L., Raveri, M., Koyama, K., Martinelli, M., Silvestri, A., Zhao, G.-B., Li, J., Peirone, S., and Zucca, A. (2022). Imprints of cosmological tensions in reconstructed gravity. *Nature Astronomy*, pages 1–7.

Pogosian, L., Silvestri, A., Koyama, K., and Zhao, G.-B. (2010). How to optimally parametrize deviations from general relativity in the evolution of cosmological perturbations. *Physical Review D*, 81(10):104023.

Popławski, N. J. (2010). Radial motion into an einstein–rosen bridge. *Physics Letters B*, 687(2-3):110–113.

Popławski, N. J. (2021). A nonsingular, anisotropic universe in a black hole with torsion and particle production. *General Relativity and Gravitation*, 53(2):1–14.

Rajpoot, S. and Vacaru, S. I. (2017). On supersymmetric geometric flows and r2 inflation from scale invariant supergravity. *Annals of Physics*, 384:20–60.

Ralston, J. P. and Jain, P. (2004). The virgo alignment puzzle in propagation of radiation on cosmological scales. *International Journal of Modern Physics D*, 13(09):1857–1877.

Reynolds, C. S. (2013). Black holes in a spin. *Nature*, 494(7438):432–433.

Reynolds, C. S. (2019). Observing black holes spin. *Nature Astronomy*, 3(1):41–47.

Reynolds, C. S. (2021). Observational constraints on black hole spin. *Annual Review of Astronomy and Astrophysics*, 59:117–154.

Riess, A. G., Yuan, W., Macri, L. M., Scolnic, D., Brout, D., Casertano, S., Jones, D. O., Murakami, Y., Anand, G. S., Breuval, L., et al. (2022). A comprehensive measurement of the local value of the hubble constant with 1 km s- 1 mpc- 1 uncertainty from the hubble space telescope and the sh0es team. *Astrophysical Journal Letters*, 934(1):L7.

Rivera, P. C. (2020). An alternative model of rotation curve that explains anomalous orbital velocity, mass discrepancy and structure of some galaxies. *American Journal of Astronomy and Astrophysics*, 7(4):73–79.

Rodrigues, D. C. (2008). Anisotropic cosmological constant and the cmb quadrupole anomaly. *Physical Review D*, 77(2):023534.

Rubin, V. C. (1983). The rotation of spiral galaxies. *Science*, 220(4604):1339–1344.

Rubin, V. C. (2000). One hundred years of rotating galaxies. *Publications of the Astronomical Society of the Pacific*, 112(772):747.

Rubin, V. C., Burstein, D., Ford Jr, W. K., and Thonnard, N. (1985). Rotation velocities of 16 sa galaxies and a comparison of sa, sb, and sc rotation properties. *Astrophysical Journal*, 289:81–98.

Rubin, V. C. and Ford Jr, W. K. (1970). Rotation of the andromeda nebula from a spectroscopic survey of emission regions. *Astrophysical Journal*, 159:379.

Rubin, V. C., Ford Jr, W. K., and Thonnard, N. (1978). Extended rotation curves of high-luminosity spiral galaxies. iv-systematic dynamical properties, sa through sc. *Astrophysical Journal*, 225:L107–L111.

Rubin, V. C., Ford Jr, W. K., and Thonnard, N. (1980). Rotational properties of 21 sc galaxies with a large range of luminosities and radii, from ngc 4605/r= 4kpc/to ugc 2885/r= 122 kpc. *Astrophysical Journal*, 238:471–487.

Rybicki, G. B. and Lightman, A. P. (2008). *Radiative processes in astrophysics*. John Wiley & Sons.

Sanders, R. (1990). Mass discrepancies in galaxies: dark matter and alternatives. *The Astronomy and Astrophysics Review*, 2(1):1–28.

Sanders, R. (1998). The virial discrepancy in clusters of galaxies in the context of modified newtonian dynamics. *Astrophysical Journal Letters*, 512(1):L23.

Sanders, R. (2012). Ngc 2419 does not challenge modified newtonian dynamics. *Monthly Notices of the Royal Astronomical Society*, 419(1):L6–L8.

Sanders, R. H. and McGaugh, S. S. (2002). Modified newtonian dynamics as an alternative to dark matter. *Annual Review of Astronomy and Astrophysics*, 40(1):263–317.

Santos, L., Cabella, P., Villela, T., and Zhao, W. (2015). Influence of planck foreground masks in the large angular scale quadrant cmb asymmetry. *Astronomy & Astrophysics*, 584:A115.

Schwarz, D. J., Starkman, G. D., Huterer, D., and Copi, C. J. (2004). Is the low-l microwave background cosmic? *PRL*, 93(22):221301.

Schwarzschild, M. (1954). Mass distribution and mass-luminosity ratio in galaxies. *Astronomical Journal*, 59:273.

Scoville, N., Abraham, R., Aussel, H., Barnes, J., Benson, A., Blain, A., Calzetti, D., Comastri, A., Capak, P., Carilli, C., et al. (2007). Cosmos: Hubble space telescope observations. *Astrophysical Journal Supplement Series*, 172(1):38.

Secrest, N. J., von Hausegger, S., Rameez, M., Mohayaee, R., Sarkar, S., and Colin, J. (2021). A test of the cosmological principle with quasars. *Astrophysical Journal Letters*, 908(2):L51.

Semenaite, A., Sánchez, A. G., Pezzotta, A., Hou, J., Scoccimarro, R., Eggemeier, A., Crocce, M., Chuang, C.-H., Smith, A., Zhao, C., et al. (2021). Cosmological implications of the full shape of anisotropic clustering measurements in boss and eboss. *Monthly Notices of the Royal Astronomical Society*, 512(4):5657–5670.

Seshavatharam, U. (2010). Physics of rotating and expanding black hole universe. *Progress in Physics*, 2:7–14.

Seshavatharam, U. and Lakshminarayana, S. (2020). An integrated model of a light speed rotating universe. *International Astronomy and Astrophysics Research Journal*, pages 74–82.

Seshavatharam, U. V. S. and Lakshminarayana, S. (2022). Concepts and results of a practical model of quantum cosmology: Light speed expanding black hole cosmology. *Mapana Journal of Sciences*, 21(2).

Shamir, L. (2011). Ganalyzer: A tool for automatic galaxy image analysis. *Astrophysical Journal*, 736(2):141.

Shamir, L. (2012). Handedness asymmetry of spiral galaxies with z¡ 0.3 shows cosmic parity violation and a dipole axis. *Physics Letters B*, 715(1):25–29.

Shamir, L. (2016). Asymmetry between galaxies with clockwise handedness and counterclockwise handedness. *Astrophysical Journal*, 823(1):32.

Shamir, L. (2017a). Large-scale photometric asymmetry in galaxy spin patterns. *Publications of the Astronomical Society of Australia*, 34:e44.

Shamir, L. (2017b). Photometric asymmetry between clockwise and counterclockwise spiral galaxies in sdss. *Publications of the Astronomical Society of Australia*, 34:e011.

Shamir, L. (2019). Cosmological-scale parity violation of galaxy spin patterns. *arXiv:1912.05429*.

Shamir, L. (2020a). Asymmetry between galaxies with different spin patterns: A comparison between cosmos, sdss, and pan-starrs. *Open Astronomy*, 29(1):15–27.

Shamir, L. (2020b). Galaxy spin direction distribution in hst and sdss show similar large-scale asymmetry. *Publications of the Astronomical Society of Australia*, 37:e053.

Shamir, L. (2020c). Patterns of galaxy spin directions in sdss and pan-starrs show parity violation and multipoles. *Astrophysics & Space Science*, 365:136.

Shamir, L. (2021a). Analysis of the alignment of non-random patterns of spin directions in populations of spiral galaxies. *Particles*, 4(1):11–28.

Shamir, L. (2021b). Large-scale asymmetry in galaxy spin directions: evidence from the southern hemisphere. *Publications of the Astronomical Society of Australia*, 38:e037.

Shamir, L. (2022a). Analysis of $\sim 10^6$ spiral galaxies from four telescopes shows large-scale patterns of asymmetry in galaxy spin directions. *Advances in Astronomy*, 2022:8462363.

Shamir, L. (2022b). Analysis of spin directions of galaxies in the desi legacy survey. *Monthly Notices of the Royal Astronomical Society*, 516(2):2281–2291.

Shamir, L. (2022c). Asymmetry in galaxy spin directions - analysis of data from des and comparison to four other sky surveys. *Universe*, 8:8.

Shamir, L. (2022d). Large-scale asymmetry in galaxy spin directions: analysis of galaxies with spectra in des, sdss, and desi legacy survey. *Astronomical Notes*, 343(6-7):e20220010.

Shamir, L. (2022e). Using machine learning to profile asymmetry between spiral galaxies with opposite spin directions. *Symmetry*, 14(5):934.

Shamir, L. (2023). Doppler shift effect as a possible explanation to the hubble-lemaitre constant tension. *Preprints: 202301.0390*.

Singal, A. K. (2019). Large disparity in cosmic reference frames determined from the sky distributions of radio sources and the microwave background radiation. *Physical Review D*, 100(6):063501.

Sivaram, C. and Arun, K. (2012). Primordial rotation of the universe, hydrodynamics, vortices and angular momenta of celestial objects. *Open Astronomy*, 5:7–11.

Sivaram, C., Arun, K., and Rebecca, L. (2020). Mond, mong, morg as alternatives to dark matter and dark energy, and consequences for cosmic structures. *Journal of Astrophysics and Astronomy*, 41(1):1–6.

Skeivalas, J., Paršeliūnas, E., and Šlikas, D. (2021). The predictive model for the universe rotation axis identification upon applying the solar system coordinate net in the milky way galaxy. *Indian Journal of Physics*, pages 1–10.

Skordis, C. and Złośnik, T. (2019). Gravitational alternatives to dark matter with tensor mode speed equaling the speed of light. *Physical Review D*, 100(10):104013.

Slipher, V. M. (1914). The detection of nebular rotation. *Lowell Observatory Bulletin*, 2:66–66.

Sofue, Y. and Rubin, V. (2001). Rotation curves of spiral galaxies. *Annual Review of Astronomy and Astrophysics*, 39:137–174.

Sommers, P. (2001). Cosmic ray anisotropy analysis with a full-sky observatory. *Astroparticle Physics*, 14(4):271–286.

Stuckey, W. (1994). The observable universe inside a black hole. *American Journal of Physics*, 62(9):788–795.

Su, S.-C. and Chu, M.-C. (2009). Is the universe rotating? *Astrophysical Journal*, 703(1):354.

Swaters, R., Sanders, R., and McGaugh, S. (2010). Testing modified newtonian dynamics with rotation curves of dwarf and low surface brightness galaxies. *Astrophysical Journal*, 718(1):380.

Takahashi, R. (2004). Shapes and positions of black hole shadows in accretion disks and spin parameters of black holes. *Astrophysical Journal*, 611(2):996.

Tatum, E. T., Seshavatharam, U., et al. (2018). Clues to the fundamental nature of gravity, dark energy and dark matter. *Journal of Modern Physics*, 9(08):1469.

Tatum, E. T., Seshavatharam, U., Lakshminarayana, S., et al. (2015a). The basics of flat space cosmology. *International journal of Astronomy and Astrophysics*, 5(02):116.

Tatum, E. T., Seshavatharam, U., Lakshminarayana, S., et al. (2015b). Flat space cosmology as a mathematical model of quantum gravity or quantum cosmology. *International journal of astronomy and astrophysics*, 5(03):133.

Tiwari, P. and Jain, P. (2015). Dipole anisotropy in integrated linearly polarized flux density in nvss data. *Monthly Notices of the Royal Astronomical Society*, 447(3):2658–2670.

Tiwari, P. and Nusser, A. (2016). Revisiting the nvss number count dipole. *JCAP*, 2016(03):062.

Trimble, V. (2009). Multiverses of the past. *Astronomical Notes*, 330(7):761–769.

Van Waerbeke, L., Mellier, Y., Erben, T., Cuillandre, J., Bernardeau, F., Maoli, R., Bertin, E., Mc Cracken, H., Fevre, O. L., Fort, B., et al. (2000). Detection of correlated galaxy ellipticities on cfht data: first evidence for gravitational lensing by large-scale structures. *Astronomy and Astrophysics*, 358:30–44.

Velten, H. and Gomes, S. (2020). Is the hubble diagram of quasars in tension with concordance cosmology? *Physical Review D*, 101(4):043502.

Vielva, P. (2010). A comprehensive overview of the cold spot. *Advances in Astronomy*, 2010.

Volonteri, M., Madau, P., Quataert, E., and Rees, M. J. (2005). The distribution and cosmic evolution of massive black hole spins. *Astrophysical Journal*, 620(1):69.

Webb, J., King, J., Murphy, M., Flambaum, V., Carswell, R., and Bainbridge, M. (2011). Indications of a spatial variation of the fine structure constant. *PRL*, 107(19):191101.

Wittman, D. M., Tyson, J. A., Kirkman, D., Dell'Antonio, I., and Bernstein, G. (2000). Detection of weak gravitational lensing distortions of distant galaxies by cosmic dark matter at large scales. *Nature*, 405(6783):143–148.

Wojnar, A., Sporea, C., and Borowiec, A. (2018). A simple model for explaining galaxy rotation curves. *Galaxies*, 6(3):70.

Wolf, M. (1914). Vierteljahresschr astron. *Ges*, 49:162.

Wu, H.-Y. and Huterer, D. (2017). Sample variance in the local measurements of the hubble constant. *Monthly Notices of the Royal Astronomical Society*, 471(4):4946–4955.

Yeung, S. and Chu, M.-C. (2022). Directional variations of cosmological parameters from the planck cmb data. *Physical Review D*, 105(8):083508.

Zhao, D. and Xia, J.-Q. (2021). A tomographic test of cosmic anisotropy with the recently-released quasar sample. *The European Physical Journal C*, 81(10):1–11.

Zhou, Y., Del Popolo, A., and Chang, Z. (2020). On the absence of a universal surface density, and a maximum newtonian acceleration in dark matter haloes: Consequences for mond. *Physics of the Dark Universe*, 28:100468.

Zwicky, F. (1937). On the masses of nebulae and of clusters of nebulae. *Astrophysical Journal*, 86:217.